Berry Phase Physics and Spin-Scattering in Time-Dependent Magnetic Fields

Bachelor Thesis

Sarah Maria Schroeter

Institute of Theoretical Physics
Faculty of Mathematics and Natural Sciences
University of Cologne

Cologne, July 6^{th} 2012

Erstgutachter:

Prof. Dr. Achim Rosch

Zweitgutachter:

Priv.-Doz. Dr. Ralf Bulla

Abstract

In 2009, a new magnetic order was observed in manganese silicide (MnSi) for specific temperatures and magnetic fields by Mühlbauer et al [1]. The study of these *skyrmions*, which are topologically stable whirls in fields, has proved to be particularly rewarding, as the coupling of the magnetic structure to electric currents is remarkably efficient.

In this Bachelor Thesis, we study the interplay of magnetism and electric current by considering the effects of a one-dimensional, non-collinear magnetic structure with a time-dependence on a passing electron moving on a ring. When an electron moves through a skyrmionic magnetic structure, its spin precesses around the direction of the local magnetic field, which leads to a change in the quantum mechanical state of the electron, expressed in the acquisition of a Berry Phase. This Berry Phase can be interpreted as a phase arising from emergent electric and magnetic fields.

In the first part of this Thesis, adiabaticity and the Berry phase are briefly introduced. We review that the Berry phase is a gauge-invariant geometric phase factor. Secondly, we compute the exact wave function of a particle moving through a non-collinear time-dependent magnetic field, which is the product of a time-dependent and an angle-dependent function.

In the next part of this Thesis, we confirm that the motion of a spin-$\frac{1}{2}$-electron through the chosen magnetic field is an adiabatic problem by showing that the exact eigenenergies in the limit of an infinite radius of the ring are in accordance with the eigenenergies emerging from an adiabatic ansatz. We then discuss Berry phase physics and find that for a time-dependence of the position of the electron, there are no emergent electric fields since the undisturbed Hamiltonian may be mapped onto a time-independent one by unitary transformations.

Finally, we allow for defects in our set-up by introducing a magnetic impurity into the system, thus breaking Galilei invariance and energy conservation. We investigate the spin-flip-rate and energy transitions of an incoming particle wave resulting from the scattering by the potential for different choices of parameters, e.g. reviewing that for large radius R, the system shows adiabatic behaviour.

Zusammenfassung

In 2009 gelang es Mühlbauer et al [1] in Mangan-Silizium (MnSi) für Temperaturen und Magnetfelder innerhalb eines bestimmten Wertebereiches eine neue magnetische Ordnung nachzuweisen. Das Studium dieser *Skyrmionen*, die, kurz gesagt, topologisch stabile Wirbel in Feldern sind, hat sich als besonders lohnenswert herausgestellt. Dies hängt vor allem mit der bemerkenswert starken Kopplung der magnetischen Struktur an elektrische Ströme zusammen.

In dieser Bachelorarbeit werden wir das Zusammenspiel von Magnetismus und elektrischen Strömen anhand eines eindimensionalen Modells näher untersuchen: Wir sind an den Effekten einer nicht-kollinearen magnetischen Struktur mit einer Zeitabhängigkeit auf ein bewegtes Elektron interessiert, das sich auf einem Ring bewegt. Bewegt sich ein Elektron durch eine magnetische Struktur, z.B. ein Skyrmion, so präzediert sein Spin um die Richtung des lokalen magnetischen Feldes, was zu einer Änderung des Quantenzustands des Elektrons führt, ausgedrückt durch die Aufnahme einer Berry-Phase. Diese Phase kann als Ergebnis emergenter elektrischer und magnetischer Felder interpretiert werden.

Im ersten Teil dieser Arbeit werden das adiabatische Theorem und die Berry-Phase kurz eingeführt. Wir überprüfen, dass die Berry-Phase invariant unter bestimmten Eichtransformationen ist und ein rein geometrischer Phasenfaktor ist. Im zweiten Teil werden wir die exakte Wellenfuntion eines Teilchens, das sich durch ein nicht-kollineares zeitabhängiges Magnetfeld bewegt, analytisch ermitteln. Diese ist ein Produkt aus einer rein zeitabhängigen und einer rein winkelabhängigen Funktion.

Im nächsten Teil dieser Arbeit werden wir überprüfen, dass die Bewegung eines Spin-$\frac{1}{2}$-Elektrons durch das gewählte magnetische Feld ein adiabatisches Problem ist, indem wir zeigen, dass die exakten Eigenenergien im Grenzfall eines unendlich großen Radius des Rings mit den Eigenenergien, die sich aus einem rein adiabatischen Ansatz ergeben, übereinstimmen. Wir werden dann die spezifische Berry-Phase berechnen und interpretieren und erkennen, dass für die gewählte Zeitabhängigkeit der Position des Elektrons sich keine emergenten elektrischen Felder ergeben. Dies hängt damit zusammen, dass das zeitabhängige Problem durch unitäre Transformationen der Schrödingergleichung auf ein zeitunabhängiges Problem abgebildet werden kann.

Im letzten Teil der Bachelorarbeit werden wir Defekte in unserem System zulassen, indem wir durch eine magnetische Störstelle die Galilei-Invarianz und Energieerhaltung brechen. Für verschiedene Parameter untersuchen wir die Spin-Flip-Rate und die Energieübergangsrate für eine einlaufende Materiewelle, die durch die Streuung an dem Potential gegeben ist. So werden wir auch nochmals bestätigen, dass sich das System für große Radien adiabatisch verhält.

Contents

1 Introduction

Magnetism may result from either a moving electric charge, i.e. electric current, or intrinsic magnetic moments. The orientation of magnetic moments, i.e. the magnetic anisotropy, arises from the coupling between the spin and the orbital angular momentum of the elementary particles in addition to the overlap of electron wave functions.

An overview of different types of magnetic order is given in figure 1. Magnetic effects can be induced by an external magnetic field. Paramagnetic and diamagnetic materials are unique, because they lack a magnetic order in the absence of a magnetic field. The resulting magnetic field inside the material is small compared to the external magnetic field. A characteristic entity is the magnetic susceptibility χ, i.e. the capability of the material to be magnetized by an external field. For diamagnetic materials, χ is negative (the diamagnet is repelled by an external field), for paramagnetic materials χ is positive. Spontaneous magnetic effects may result from exchange interaction, i.e. the overlap of electron wave functions, as it is the case with ferro- and anti-ferromagnetic structures, which posses relatively large magnetic moments.

A particularly interesting form of magnetic order is present in chiral magnets. These are

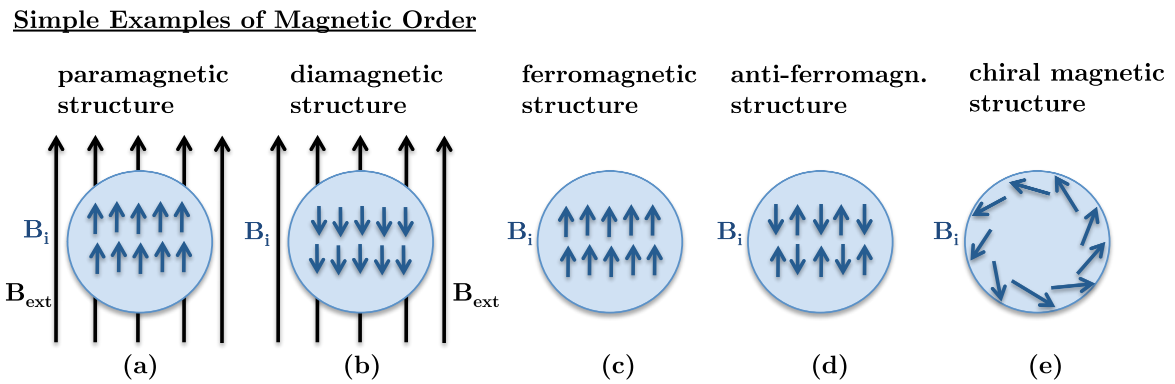

Figure 1: (a) Paramagnets have intrinsic magnetic moments which align themselves in the direction of an externally applied magnetic field. As a result, the overall magnetic field is reinforced. (b) For diamagnets it is most energy-efficient for magnetic moments to align themselves antiparallel to the external magnetic field. The resulting magnetic field is weakened. (c) Ferromagnets show a spontaneous magnetization, a net magnetic moment, resulting from the spin and orbital movement of an electron from a partially filled shell. As the dipoles align spontaneously and tendentially parallel to each other, there is a magnetization even when no external magnetic field is applied. (d) In an antiferromagnet, neighbouring electrons are inclined to point in opposite directions, i.e. the total magnetization vanishes. If, however, a magnetic field is applied, one observes a net magnetization different from zero. (e) Chiral magnetic structures emerge from asymmetric spin-interactions. Their mirrored image cannot be converted to the original by simple rotations or translations. Thus, they possess the attribute of handedness [2].

magnetic structures, whose mirrored image cannot be converted to the original by simple rotations or translations and thus have an additional attribute: handedness. Where locally the order of the atoms in the solid possesses no center of inversion, spin-orbit coupling can lead to asymmetric components of interactions and electronic properties (although much weaker than normal exchange-interaction) [3].

An intriguing example emerging from asymmetric spin-interactions are skyrmion lattices. 1989 Alexey Bogdanov predicted that for anisotropic chiral magnets there is a new magnetic order consisting of topologically stable spin whirls, named skyrmions after the English particle physicist Tony Skyrme, who showed that localized solutions to non-linear quantum field theories may be interpreted as elementary particles. Briefly speaking, skyrmions are topologically stable whirls in fields.

In 2009, a new magnetic order was observed in manganese silicide (MnSi) for specific temperatures and magnetic fields by Mühlbauer et al [1]. Evidence for the existence of skyrmions has been provided using neutron scattering by the experimental research group of Christian Pfleiderer in collaboration with the theory group of Achim Rosch [4]. Since 2009, the skyrmion lattice has been further studied and methods of detecting this magnetic order have been extended. Not only has the skyrmion lattice been observed in metals such as MnSi, but it has recently also been observed in semiconductors and insulating materials [5–8].

When an electron moves through a skyrmionic magnetic structure, its spin precesses around the direction of the local magnetic field, which leads to a change in the quantum mechanic state of the electron, expressed in the acquisition of a Berry Phase (cf. figure 2). This Berry Phase may be interpreted as a phase arising from emergent electric and magnetic fields when assuming the electron moves through a uniform magnetic field [9–12]. Investigating these emergent electric and magnetic fields of an interacting electron and a skyrmion lattice is particularly rewarding for numerous reasons. For example, in conventional magnets, the winding number W per magnetic unit cell is equal to zero, while in a skyrmion lattice W is finite and quantized, $W = -1$. As a result, the emergent magnetic fields (or, more specifically, the emergent flux) are also quantized.

The physics of an electron moving through the magnetic field can be analyzed from two different points of view:
From the point of view of the electron, i.e. considering the problem in terms of emergent electic and magnetic fields, the change in spin orientation is equal to an effective Lorentz force acting on the electron, which is perpendicular to its motion [13]. As a result, the magnetic field induces a deflection of the electron, which can be measured by making use of the topological Hall-effect [14]. Because of the electron carrying an electric charge, a potential may be measured perpendicular to the direction of the current. Since the magnetic structure of the Skyrmion lattice is very smooth, the adjustment of the spin of the electron to the magnetization of the skyrmion lattice can be considered an adiabatic process.

On the other hand, there must be a corresponding counter-force acting on the skyrmion. This force, arising from the transfer of angular momentum from the conduction electrons to the local magnetic structure (cf. [15]), can for example result in a drift of the domains of the lattice.

Skyrmions are exceptionally suitable structures when studying the interplay of electric currents and magnetization, a subject from the field of spintronics, as they are particularly sensitive to current densities of about 10^6 A/m^2, which is far below the magnitude needed to induce similar effects in other magnetic textures such as domain walls [16, 17].

A 1D model of an electron passing over a static magnetic field has previously been investigated in the Bachelor thesis of M. Baedorf [18].

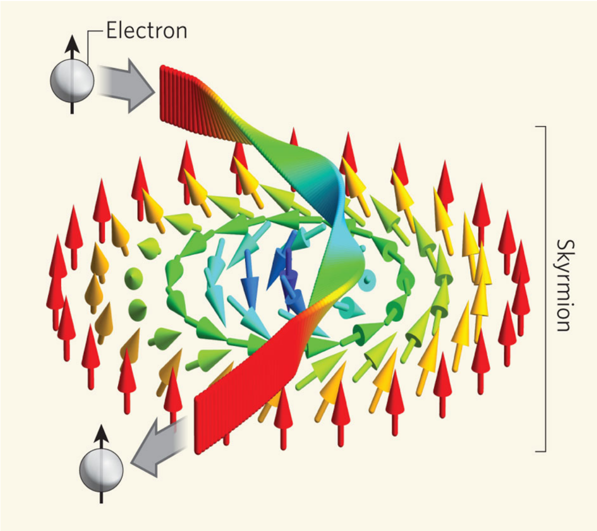

Figure 2: When an electron moves through a non-collinear magnetic field, it acquires a quantum mechanical phase, the Berry Phase, which results from the adiabatic adaptation of the spin to the magnetic structure. The change of spin orientation results in an effective Lorentz force deflecting the electron. From [13].

In this thesis, we investigate the effects of a one dimensional, non-collinear magnetic structure with a translational linear time-dependence on a passing electron moving on a ring. In particular, we are interested in observing emergent electrodynamics and whether the interaction of the spin of the particle with the underlying time-dependent magnetic field leads to emergent electric fields.

Firstly, adiabaticity and the Berry phase are concisely introduced (Section 2). Secondly, in Section 3 we will compute the exact wave function of a particle moving through a non-collinear time-dependent magnetic field.

In the subsequent part, we will establish that the motion of a spin-$\frac{1}{2}$-electron through the chosen magnetic field is an adiabatic problem by comparing the exact eigenenergies in the limit of an infinite radius of the ring with the eigenenergies emerging from an adiabatic ansatz. Section 5 will then explore possible Berry phase physics and investigate whether there are emergent electric and magnetic fields. In order to investigate the relevance of our choice of time-dependence for the emergence of new physics, we will consider Galilean invariance in Section 6.

In Section 7, we will allow for defects in our set-up by introducing a magnetic impurity into the system. We will investigate the spin-flip-rate and energy transitions of an incoming particle wave resulting from the scattering by the potential.

2 The Berry Phase

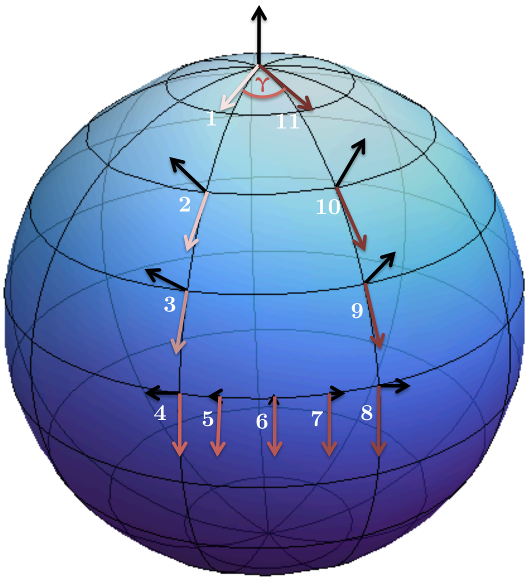

Figure 3: The geometric analogon to the Berry phase is a parallel transport of a vector, e.g. on the surphace of a sphere: When a vector in the tangent space to the manifold is transported parallely along a smooth, closed curve in a manifold, e.g. on the surface of a sphere, the resulting angle γ between the initial and the final vector is proportional to the area enclosed by the curve.

The Berry Phase was first described by Sir Michael Berry in 1984. In this section we will revise the essentials of his derivations which can also be found in his original paper (cf. [19]) and further detail their implications as well as their relations to the adiabatic theorem. The Berry Phase is a gauge-invariant geometric phase, which is gathered by the wave function when tracing out a closed curve in parameter space provided the change is adiabatic. We denote the set of parameters as $\mathbf{r}(t)$, i.e. a closed curve corresponds to the condition $\mathbf{r}(t_0) = \mathbf{r}(t_0 + T)$.

Adiabatic processes constitute the limiting case between statics and dynamics. Generally, adiabatic processes are processes which occur extremely slowly (over a long period of time). More precisely, adiabatic change in quantum mechanics can be defined as a process in which no transitions between different eigenstates occur [20].

The Berry Phase is, as we will later determine, purely geometrical, i.e. does not depend on the velocity with which the cycle is performed.

2.1 The Adiabatic Theorem of Quantum Mechanics

Consider a time-dependent Hamiltonian in a parameter space varying with time, $H = H(\mathbf{r}(t))$, and a corresponding discrete and non-degenerate spectrum of eigenenergies:

$$H(\mathbf{r}(t))\,|n(\mathbf{r}(t))\rangle = E_n(\mathbf{r}(t))\,|n(\mathbf{r}(t))\rangle.$$

where $E_n(\mathbf{r}(t))$ is the time-evolved eigenenergy corresponding to H.

We are concerned with investigating the motion of the particle along a closed path C in parameter space where H is periodic in time, i.e. $H(\mathbf{r}(t_0)) = H(\mathbf{r}(t_0 + T))$. As an example, we might consider a free particle whose energy might vary depending on its time-dependent position $\mathbf{r}(t) = (x(t), y(t), z(t))$

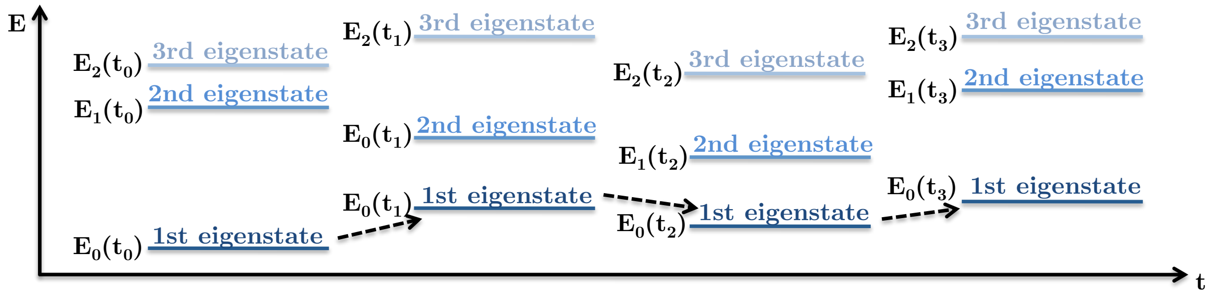

Figure 4: Initially, let the system be in an eigenstate of the Hamiltonian H. When change occurs adiabatically, the system does not perform any transitions into any other fundamental eigenstate, although the evolved eigenenergy (or the amplitude of the wave function) may vary with time.

Assume a system initially is in the n-th eigenstate of the Hamiltonian H, $|\,\psi(\mathbf{r}(0))\rangle = |n(\mathbf{r}(0))\rangle$. The adiabatic theorem states that if H changes adiabatically, $|\,\psi(\mathbf{r}(t))\rangle$ stays in the time-evolved n-th eigenstate of H. The system does not perform any transitions into other eigenstates, although the eigenenergy may vary with time, compare figure 4.

Slow evolvement of H allows the ansatz $|\,\psi_n(t)\rangle = c_n(t)\,|\,n(\mathbf{r}(t))\rangle$, where $c_n(t)$ are time-dependent prefactors. Plugging this ansatz into the Schroedinger equation and projecting the result onto the eigenstate $\langle n(\mathbf{r}(t))\,|$ yields:

$$
\begin{aligned}
\langle n(\mathbf{r}(t))\,|\,i\hbar\frac{d}{dt}\left[c_n(t)\,|\,n(\mathbf{r}(t))\rangle\right] =& \langle n(\mathbf{r}(t))\,|\left(i\hbar\frac{d}{dt}c_n(t)\right)|\,n(\mathbf{r}(t))\rangle + \langle n(\mathbf{r}(t))\,|\,c_n(t)i\hbar\frac{d}{dt}\,|\,n(\mathbf{r}(t))\rangle \\
=& i\hbar\frac{d}{dt}c_n(t) + \langle n(\mathbf{r}(t))\,|\,i\hbar\frac{d}{dt}\,|\,n(\mathbf{r}(t))\rangle c_n(t) \overset{!}{=} E_n(t)\cdot c_n(t) \\
\Rightarrow\quad \dot{c}_n(t) =& \left(-\langle n(\mathbf{r}(t))\,|\,\frac{d}{dt}\,|\,n(\mathbf{r}(t))\rangle - \frac{i}{\hbar}E_n(\mathbf{r}(t))\right)c_n(t), \quad \text{where } \dot{c}_n = \frac{d}{dt}c_n \\
=& \left(-\langle n(\mathbf{r}(t))\,|\,\nabla_{\mathbf{r}}\,|\,n(\mathbf{r}(t))\rangle\dot{\mathbf{r}}(t) - \frac{i}{\hbar}E_n(\mathbf{r}(t))\right)c_n(t)
\end{aligned}
$$

The time-dependent prefactors may now be written as

$$
c_n(t) = \exp\left(-\frac{i}{\hbar}\int_{t_0}^{t}\left\{E_n(\mathbf{r}(t')) - i\hbar\langle n(\mathbf{r}(t))\,|\,\nabla_{\mathbf{r}}\,|\,n(\mathbf{r}(t))\rangle\dot{\mathbf{r}}(t)\right\}dt'\right) \tag{1}
$$

where $\exp\left(-\frac{i}{\hbar}\int_{t_0}^{t}E_n(\mathbf{r}(t'))dt'\right)$ is known as the dynamic phase factor and

$$
\gamma_n(t) = i\oint_C \langle n(\mathbf{r}(t))\,|\,\nabla_{\mathbf{r}}\,|\,n(\mathbf{r}(t))\rangle d\mathbf{r} \tag{2}
$$

is the Berry Phase.

Consequently, the time evolved wave function is given by

$$|\psi(t)\rangle = \exp\left(-\frac{i}{\hbar}\int_0^t E_n(\mathbf{r}(t'))dt'\right) e^{i\gamma_n(t)}|n(\mathbf{r}(t))\rangle$$

where $e^{i\gamma_n(t)}$ is the geometric phase factor.

Until 1984, this additional phase factor was neglected, because it vanishes under gauge-transformations under certain conditions. However, when considering the motion of a particle along a closed loop in parameter space, the Berry phase can no longer be neglected and non-negligible quantum physical attributes emerge.

2.2 Characteristics of the Berry Phase

Clearly, Berry's Phase is a purely geometric phase, i.e. it is only path-dependent, while impervious to the velocity with which the path is traced out adiabatically.
Rewriting the Berry Phase, we can define the following additional interdependent physical entities (cf. [21]):

$$\begin{aligned}\gamma_n(t) =& i\oint_C \langle n(\mathbf{r}(t))|\nabla_{\mathbf{r}}|n(\mathbf{r}(t))\rangle d\mathbf{r}\\ =& \oint_C \underbrace{A_n(\mathbf{r})}_{\equiv \text{ Berry Connection}} d\mathbf{r} = \int_S \underbrace{\nabla \times A_n(\mathbf{r})}_{\equiv \text{ Berry Curvature}} d\mathbf{S} = i\int_S \nabla \times \langle n|\nabla|n\rangle\, d\mathbf{S}\end{aligned}$$

The Berry phase $\gamma_n(t)$ is a real number, because

$$\begin{aligned}\langle n|n\rangle = 1 \text{ (normalized)} \Rightarrow& \langle n|\nabla|n\rangle + \langle\nabla n|n\rangle = 0\\ \Rightarrow& \langle\nabla n|n\rangle = -\langle n|\nabla|n\rangle = -\overline{\langle\nabla n|n\rangle} \Rightarrow \langle n|\nabla|n\rangle \in i\mathbb{R}\end{aligned}$$

As mentioned above, the Berry-Phase is gauge-invariant under the transformation

$$|n\rangle \longrightarrow |\tilde{n}\rangle = e^{i\gamma_n(\mathbf{r})}|n\rangle.$$

This can be proven by considering the Berry connection.
The transformation $|n\rangle \longrightarrow |\tilde{n}\rangle$ results in a transformation

$$\begin{aligned}A_n(\mathbf{r}) \longrightarrow \tilde{A}_n(\mathbf{r}) =& i\langle n|e^{-i\gamma_n(\mathbf{r})}\nabla_{\mathbf{r}}e^{i\gamma_n(\mathbf{r})}|n\rangle\\ =& \nabla_{\mathbf{r}}\gamma_n(\mathbf{r}) + i\langle n|\nabla_{\mathbf{r}}|n\rangle = \nabla_{\mathbf{r}}\gamma_n(\mathbf{r}) + A_n(\mathbf{r})\end{aligned}$$

and thus the Berry phase moves on to

$$\gamma_n(t) \longrightarrow \tilde{\gamma}_n(t) = \int_S (\nabla \times \tilde{A}_n(\mathbf{r}))d\mathbf{S} = \int_S (\nabla \times A_n(\mathbf{r}))d\mathbf{S} = \gamma_n(t)$$

where in the last line we have made use of the fact that the rotation of a gradient of a scalar function vanishes, $\nabla \times (\nabla \phi) = 0$.

The physical implications of the Berry phase can be understood when considering its interpretation as a gauge potential. We will further elaborate on these properties in Section 4.2.1.

3 Spin-$\frac{1}{2}$-Particle in a Time-Dependent Magnetic Field

3.1 Set-Up

The Berry Phase may be observed in many different contexts of quantum mechanics. In the following, we will study the behaviour of a spin-$\frac{1}{2}$ particle, more specifically an electron with mass m_e, when passing through a magnetic field with a fixed strength B_0. We restrict the motion of a particle to a one-dimensional wire, or rather a ring with radius R, thus assuming periodic boundary conditions. In particular, we will focus on magnetic fields evolving adiabatically in time. Figure 5 shows the intellectual set-up. We express the magnetic field as a function of angles ϕ and θ, i.e. only the direction of the magnetic field vectors change while the strength B_0 is kept fixed. ϕ sets the position where the particular magnetic field is measured. At every position ϕ on the border of the circle we attach an imaginary 3D-sphere which determines the direction of the field vector. In effect, the magnetic field is constituted by mere spherical coordinates. In addition, we allow variation of both angles ϕ and θ in time with a frequency of ω_1 and ω_2 respectively.

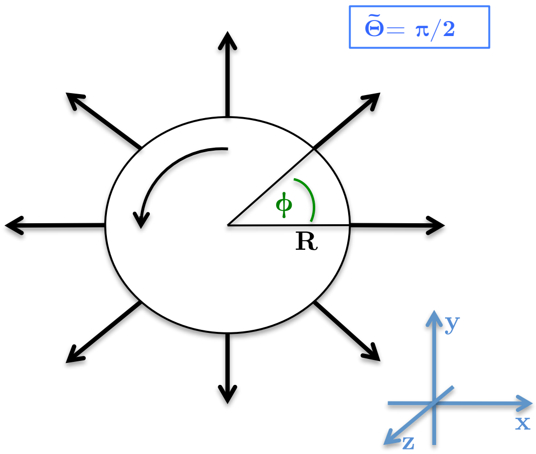

$$\begin{aligned}
\mathbf{B}(\mathbf{r},t) &= B_0\hat{\mathbf{n}}(\phi,\theta,t) \\
&= B_0 \begin{pmatrix} \sin(\theta-\omega_2 t)\cos(\phi-\omega_1 t) \\ \sin(\theta-\omega_2 t)\sin(\phi-\omega_1 t) \\ \cos(\theta-\omega_2 t) \end{pmatrix} \\
&= B_0 \begin{pmatrix} \sin(\tilde{\theta})\cos(\tilde{\phi}) \\ \sin(\tilde{\theta})\sin(\tilde{\phi}) \\ \cos(\tilde{\theta}) \end{pmatrix} \qquad (3)
\end{aligned}$$

where $\tilde{\phi} = \phi - \omega_1 t$ and $\tilde{\theta} = \theta - \omega_2 t$.

Figure 5: For $\tilde{\theta} = \pi/2$, the magnetic field is cylindrically symmetrical

As an example, an angle $\tilde{\theta} = 0$ means that the magnetic field vectors all point out of the paper plane, $\mathbf{B} = B_0(0,0,1)^T$, corresponding to a ferromagnetic structure. Figure 5 shows the situation for an angle of $\theta = \pi/2$, where $\mathbf{B} = B_0(\cos(\tilde{\phi}), \sin(\tilde{\phi}), 0)^T$.

The Hamiltonian is made up of a kinetic part and a part arising from the interaction of the particle with the magnetic field:

$$\mathbf{H}_0(\mathbf{r},t) = \frac{\hat{p}^2}{2m_e} + \mathbf{B}(\mathbf{r},t) \cdot \frac{g_S|\mu_B|}{\hbar}\mathbf{S}, \quad \text{where } |\mu_B| = \frac{|e|\hbar}{2m_e} \qquad (4)$$

The spin operator $\mathbf{S}$ is proportional to the vector of pauli matrices $\boldsymbol{\sigma}$:

$$\mathbf{S} = \frac{\hbar}{2}\boldsymbol{\sigma}, \quad \boldsymbol{\sigma} = (\boldsymbol{\sigma}_x, \boldsymbol{\sigma}_y, \boldsymbol{\sigma}_z), \quad \boldsymbol{\sigma}_x = \begin{pmatrix} 0 & 1 \\ 1 & 0 \end{pmatrix}, \boldsymbol{\sigma}_y = \begin{pmatrix} 0 & -i \\ i & 0 \end{pmatrix}, \boldsymbol{\sigma}_z = \begin{pmatrix} 1 & 0 \\ 0 & -1 \end{pmatrix} \tag{5}$$

as a result, considering that for an electron $g_S = 2$, we may write

$$\mathbf{H}_0(\mathbf{r}, t) = \frac{\hat{p}^2}{2m_e} + |\mu_B| \mathbf{B}(\mathbf{r}, t) \cdot \boldsymbol{\sigma} \tag{6}$$

We will be denoting the wave function of the particle as

$$\psi(\mathbf{r}, t) = \begin{pmatrix} u_1(\mathbf{r}, t) \\ u_2(\mathbf{r}, t) \end{pmatrix} \tag{7}$$

3.2 Generating Rotational and Translational Invariance

We will now simplify the calculation of eigenfunctions of $\mathbf{H}_0$ and eigenenergies by determining eigenfunctions of an operator which commutes with $\mathbf{H}_0$ and, at the same time, determine the associated law of conservation.

Note that an observable $\mathbf{A}$ satisfies the law of conservation if

$$_t\langle\psi\,|\,\mathbf{A}\,|\,\psi\rangle_t = \text{const.} \;\Leftrightarrow\; [\mathbf{A}, \mathbf{H}] = 0 \;\Leftrightarrow\; e^{\frac{i}{\hbar}\mathbf{A}\alpha}\mathbf{H}e^{-\frac{i}{\hbar}\mathbf{A}\alpha} = \mathbf{H} \tag{8}$$

i.e. $\mathbf{A}$ is constant over time and $\mathbf{H}$ is invariant under every transformation generated by the observable $\mathbf{A}$, see [22].

In order to find an operator which might be suitable to commute with our Hamiltonian $\mathbf{H}_0$, we ask ourselves which operator $\mathbf{A}$ satisfies $_t\langle\psi\,|\mathbf{A}|\,\psi\rangle_t = \text{const.}$ (and thus $[\mathbf{A}, \mathbf{H}] = 0$). This must be an operator which generates rotational and translational invariance, i.e. which reverses a combination of a translational shift and a rotation of the spinor.

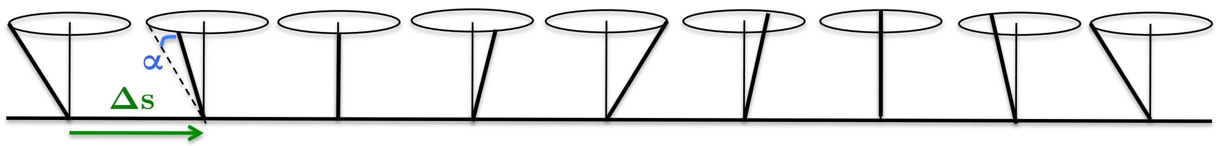

Translate by Δs = R $\Delta\phi$, rotate spinor by an angle α

Figure 6: A change of position corresponds to a combination of a translational shift $\Delta s = R\Delta\phi$ and a rotation of the spinor by an angle α

Translations in position-space by $\Delta\mathbf{s}$:

A translation operator $\hat{\mathbf{T}}_{\Delta\mathbf{s}}$ is trivially expected to cause a translation $\Delta\mathbf{s}$ in position-space, so that

$$\tilde{\psi}(\mathbf{r}) = \hat{\mathbf{T}}_{\Delta\mathbf{s}}\psi(\mathbf{r}) = \psi(\mathbf{r} - \Delta\mathbf{s}) \tag{9}$$

Taylor expanding this expression for small $\Delta\mathbf{s}$ around $\Delta\mathbf{s} = 0$ yields:

$$\psi(\mathbf{r} - \Delta\mathbf{s}) = \psi(\mathbf{r}) - \Delta\mathbf{s} \cdot \nabla\psi(\mathbf{r}) + \mathcal{O}(\Delta\mathbf{s}^{\ 2})$$

$$\Rightarrow \hat{\mathbf{T}}_{\Delta\mathbf{s}} = \mathbb{1} - \Delta\mathbf{s} \cdot \nabla = \mathbb{1} - \Delta\mathbf{s}\frac{i}{\hbar}\mathbf{p}, \quad \text{with } \mathbf{p} = \frac{\hbar}{i}\nabla = \frac{\hbar}{iR}\partial_{\tilde{\phi}}$$

When considering consecutive infinitesimal translational shifts, we get

$$\hat{\mathbf{T}}_{\Delta\mathbf{s}} = \lim_{N\to\infty}(\hat{\mathbf{T}}_{\Delta\mathbf{s}/N})^N = \lim_{N\to\infty}(\mathbb{1} - \frac{\Delta\mathbf{s}}{N}\frac{i}{\hbar}\mathbf{p})^N = e^{-\frac{i}{\hbar}\Delta\mathbf{s}\cdot\mathbf{p}} \tag{10}$$

where we have made use of the identity $\lim_{N\to\infty}(1 - \frac{x}{N})^N = e^{-x}$.
Consequently, we have reviewed that $\mathbf{p} = \frac{\hbar}{i}\nabla$ generates a translation by $\Delta\mathbf{s}$.

Rotation of a spinor by an angle α:

We will now find the representation of an operator generating the rotation of a spinor by an angle α. To this end, consider the form assumed by a vector (x, y) when rotated by an angle α to a position (x', y').

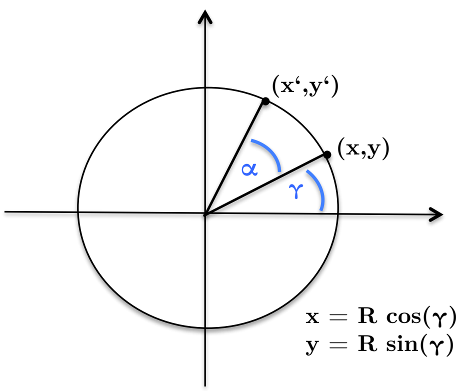

$$\begin{aligned}
\begin{pmatrix} x' \\ y' \end{pmatrix} &= \begin{pmatrix} R\cdot\cos(\alpha+\gamma) \\ R\cdot\sin(\alpha+\gamma) \end{pmatrix} \\
&= \begin{pmatrix} R(\cos\alpha\cos\gamma - \sin\alpha\sin\gamma) \\ R(\sin\alpha\cos\gamma + \cos\alpha\sin\gamma) \end{pmatrix} \\
&= \begin{pmatrix} \cos\alpha & -\sin\alpha \\ \sin\alpha & \cos\alpha \end{pmatrix}\begin{pmatrix} x \\ y \end{pmatrix} \\
&\underset{\alpha\ll 1}{\approx} \begin{pmatrix} 1 & -\alpha \\ \alpha & 1 \end{pmatrix}\begin{pmatrix} x \\ y \end{pmatrix} = \begin{pmatrix} x - y\alpha \\ y + x\alpha \end{pmatrix}
\end{aligned}$$

Figure 7: Rotation of the spinor (x, y) by an angle α yields the vector (x', y')

Let us now consider the effect of a rotation operator $\hat{A}_{\alpha,z}$ on the wave function:

$$\tilde{\psi}(\mathbf{r}) = \hat{\mathbf{A}}_{\alpha,z}\psi(\mathbf{r}) = \psi(x - \alpha y, y + \alpha x, z) \tag{11}$$

$$\approx \psi(\mathbf{r}) - \alpha y\partial_x\psi(\mathbf{r}) + \alpha x\partial_y\psi(\mathbf{r}) \qquad (\text{for } \alpha \ll 1) \tag{12}$$

$$= (\mathbb{1} + \frac{i}{\hbar}\alpha\mathbf{S}_z)\ \psi(\mathbf{r}), \quad \text{where } \mathbf{L}_z = \frac{\hbar}{iR}x\partial_y - \frac{\hbar}{iR}y\partial_x = xp_y - yp_x \tag{13}$$

This is the operator generating rotations in position space. However, we are interested in rotations in spin space which is generated by the orthonormal basis $\left\{ |\uparrow\rangle \simeq \begin{pmatrix} 1 \\ 0 \end{pmatrix}, |\downarrow\rangle \simeq \begin{pmatrix} 0 \\ 1 \end{pmatrix} \right\}$, so that a general state is given by $\begin{pmatrix} a_1 \\ a_2 \end{pmatrix} = a_1 |\uparrow\rangle + a_2 |\downarrow\rangle$. The spin momentum operator $\mathbf{S}_z$ is defined as the very operator which generates these spinor rotations so that

$$\mathbf{S}_z |\uparrow\rangle = \frac{\hbar}{2R} |\uparrow\rangle, \quad \mathbf{S}_z |\downarrow\rangle = -\frac{\hbar}{2R} |\downarrow\rangle \quad \text{where } \mathbf{S}_z = \frac{\hbar}{2R} \boldsymbol{\sigma}_z \tag{14}$$

Consecutive application of many infinitesimal rotational shifts produces:

$$\hat{\mathbf{A}}_{\alpha,z} = e^{-\frac{i}{\hbar}\alpha \mathbf{S}_z} \tag{15}$$

Note that for a general rotation about the axis $\frac{\boldsymbol{\alpha}}{\alpha}$ we have $\hat{\mathbf{A}}_{\boldsymbol{\alpha}} = e^{-\frac{i}{\hbar}\boldsymbol{\alpha}\mathbf{S}}$, where $\mathbf{S} = (\mathbf{S}_x, \mathbf{S}_y, \mathbf{S}_z)$ and $\mathbf{S}_i = \frac{\hbar}{2}\boldsymbol{\sigma}_i$ [22].

Thus we have reviewed that $\mathbf{S}_z$ generates a rotation in spin space by an angle α about the z-axis.

Result:

Combining the operators generating the translation and the rotation gives

$$\mathbf{g} = -i\hbar \frac{\partial}{\partial s} \mathbb{1} + \frac{\hbar}{2R} \boldsymbol{\sigma}_z = -\frac{i\hbar}{R} \frac{\partial}{\partial \tilde{\phi}} \mathbb{1} + \frac{\hbar}{2R} \boldsymbol{\sigma}_z, \qquad \tilde{\mathbf{g}} = -i \frac{\partial}{\partial \tilde{\phi}} \mathbb{1} + \frac{\boldsymbol{\sigma}_z}{2} = \tilde{p}\mathbb{1} + \frac{\boldsymbol{\sigma}_z}{2} \tag{16}$$

where $\tilde{\mathbf{g}}$ is a rescaled version of $\mathbf{g}$ (please note that, in the following, identity matrices will be left out where appropriate for the purpose of simplifying the notation).
The resulting operator generates translational and rotational invariance combined, i.e.

$$\tilde{\psi}(\mathbf{r}) = \hat{\mathbf{T}}_{\Delta\mathbf{s}} \hat{\mathbf{A}}_{\alpha,z} \psi(\mathbf{r}) = e^{-\frac{i}{\hbar}\Delta\mathbf{s}\cdot\mathbf{p}} e^{-\frac{i}{\hbar}\alpha\mathbf{S}_z} \psi(\mathbf{r}) \stackrel{!}{=} \text{const.} \cdot \psi(\mathbf{r}) \tag{17}$$

Consider

$$\mathbf{H}_0(\mathbf{r}, t) = \frac{\hat{p}^2}{2m} + \mathbf{B}(\mathbf{r}, t) \cdot \frac{g_S |\mu_B|}{\hbar} \mathbf{S} \tag{18}$$

We confine ourselves to the xy-plane, with the real space parameter $\theta = \frac{\pi}{2}$ and R kept fixed. The nabla-operator can in this case be simplified to be:

$$\nabla = \hat{\mathbf{e}}_r \frac{\partial}{\partial r} + \hat{\mathbf{e}}_\theta \frac{1}{R} \frac{\partial}{\partial \tilde{\theta}} + \hat{\mathbf{e}}_{\tilde{\phi}} \frac{1}{R \sin\theta} \frac{\partial}{\partial \tilde{\phi}} \quad \Rightarrow \quad \nabla^2 = \left(\frac{1}{R} \frac{\partial}{\partial \tilde{\phi}} \right)^2 \tag{19}$$

Thus we can rewrite the Hamiltonian $\mathbf{H}_0$ as

$$\mathbf{H}_0 = -\frac{\hbar^2}{2mR^2}\left(\frac{\partial}{\partial\tilde{\phi}}\right)^2 + |\mu_B|\,\mathbf{B}_0(\mathbf{r},t)\boldsymbol{\sigma} \tag{20}$$

$$= \frac{\hbar^2}{mR^2}\left(-\frac{1}{2}\left(\frac{\partial}{\partial\tilde{\phi}}\right)^2 + \underbrace{\frac{|\mu_B|\,B_0}{\hbar^2/mR^2}}_{=:\alpha}\hat{\mathbf{n}}\boldsymbol{\sigma}\right) \tag{21}$$

$$= \frac{\hbar^2}{mR^2}\left(-\frac{1}{2}\left(\frac{\partial}{\partial\tilde{\phi}}\right)^2 + \alpha\hat{\mathbf{n}}\boldsymbol{\sigma}\right) = \frac{\hbar^2}{mR^2}\tilde{\mathbf{H}}_0 \tag{22}$$

We can prove that, as intended by our careful construction of $\mathbf{g}$, $\tilde{\mathbf{H}}_0$ and $\tilde{\mathbf{g}}$ and consequently $\mathbf{H}_0$ and $\mathbf{g}$ do indeed commute.

$$\left[\tilde{\mathbf{H}}_0, \tilde{\mathbf{g}}\right] = \left[-\frac{1}{2}\left(\frac{\partial}{\partial\tilde{\phi}}\right)^2 + \alpha\hat{\mathbf{n}}\boldsymbol{\sigma}, -i\frac{\partial}{\partial\tilde{\phi}} + \frac{\boldsymbol{\sigma}_z}{2}\right] \tag{23}$$

$$= \left[-\frac{1}{2}\left(\frac{\partial}{\partial\tilde{\phi}}\right)^2, -i\frac{\partial}{\partial\tilde{\phi}}\right] + \left[\alpha\hat{\mathbf{n}}\boldsymbol{\sigma}, -i\frac{\partial}{\partial\tilde{\phi}}\right] + \left[-\frac{1}{2}\left(\frac{\partial}{\partial\tilde{\phi}}\right)^2, \frac{\boldsymbol{\sigma}_z}{2}\right] + \left[\alpha\hat{\mathbf{n}}\boldsymbol{\sigma}, \frac{\boldsymbol{\sigma}_z}{2}\right] \tag{24}$$

$$= i\alpha\left(\frac{\partial}{\partial\tilde{\phi}}\hat{\mathbf{n}}\boldsymbol{\sigma}\right) + \frac{\alpha\hat{\mathbf{n}}}{2}\left([\boldsymbol{\sigma}_x,\boldsymbol{\sigma}_z],[\boldsymbol{\sigma}_y,\boldsymbol{\sigma}_z],[\boldsymbol{\sigma}_z,\boldsymbol{\sigma}_z]\right) \tag{25}$$

$$\text{with } [\boldsymbol{\sigma}_i,\boldsymbol{\sigma}_j] = 2i\epsilon_{ijk}\boldsymbol{\sigma}_k \tag{26}$$

$$= i\alpha\left(\frac{\partial}{\partial\tilde{\phi}}(\sin\tilde{\theta}\cos\tilde{\phi}\;\boldsymbol{\sigma}_x + \sin\tilde{\theta}\sin\tilde{\phi}\;\boldsymbol{\sigma}_y + \cos\tilde{\theta}\;\boldsymbol{\sigma}_z)\right) + i\alpha\hat{\mathbf{n}}(-\boldsymbol{\sigma}_y,\boldsymbol{\sigma}_x,0) \tag{27}$$

$$= i\alpha(-\sin\tilde{\theta}\sin\tilde{\phi}\;\boldsymbol{\sigma}_x + \sin\tilde{\theta}\cos\tilde{\phi}\;\boldsymbol{\sigma}_y) + i\alpha\hat{\mathbf{n}}(-\boldsymbol{\sigma}_y,\boldsymbol{\sigma}_x,0) \tag{28}$$

$$= 0 \tag{29}$$

We have thus shown that $\tilde{\mathbf{H}}_0$ and $\tilde{\mathbf{g}}$ possess the same system of eigenfunctions. Moreover, according to equation (8), the sum of momentum and angular momentum is a conserved quantity. In the following, we will regard $\tilde{\mathbf{g}}$ as a generalized momentum operator.

3.3 Solution to the Momentum-Operator

We will now establish the eigenfunctions of $\tilde{\mathbf{g}}$ solving the eigensystem

$$\left(-i\frac{\partial}{\partial\tilde{\phi}}\mathbb{1} + \frac{\boldsymbol{\sigma}_z}{2}\right)|\psi\rangle = K\,|\psi\rangle \tag{30}$$

$$-i\frac{\partial}{\partial\tilde{\phi}}\mathbb{1}\,|\psi\rangle = \left(K - \frac{\boldsymbol{\sigma}_z}{2}\right)|\psi\rangle = \begin{pmatrix} (K-\frac{1}{2}) & 0 \\ 0 & (K+\frac{1}{2}) \end{pmatrix}|\psi\rangle \tag{31}$$

with eigenvalues

$$\lambda_{1/2} = (K \mp \frac{1}{2}) \tag{32}$$

and respective eigenfunctions

$$|\,\psi_1\rangle = \begin{pmatrix} 1 \\ 0 \end{pmatrix} e^{i(K-\frac{1}{2})\phi} = \begin{pmatrix} \psi_1 \\ 0 \end{pmatrix} \tag{33}$$

$$|\,\psi_2\rangle = \begin{pmatrix} 0 \\ 1 \end{pmatrix} e^{i(K+\frac{1}{2})\phi} = \begin{pmatrix} 0 \\ \psi_2 \end{pmatrix} \tag{34}$$

As we study the motion of a particle on a ring, we require $|\,\psi(\phi)\rangle$ to fulfill periodic boundary conditions:

$$|\,\psi(\tilde{\phi})\rangle = |\,\psi(\tilde{\phi}+2\pi)\rangle \Rightarrow e^{i(K\mp\frac{1}{2})2\pi} = 1 \Rightarrow K = n + \frac{1}{2},\ n \in \mathbb{Z} \tag{35}$$

This means that the momentum is quantized.
The general solution to equation (30) is a linear combination of both eigenfunctions:

$$|\,\psi\rangle = c_1(t)\,|\,\psi_1\rangle + c_2(t)\,|\,\psi_2\rangle = \begin{pmatrix} c_1(t)\psi_1 \\ c_2(t)\psi_2 \end{pmatrix} \tag{36}$$

where $c_1(t)$ and $c_2(t)$ do not depend on ϕ.

3.4 Solution to the Time-Dependent Hamiltonian

Ultimately, we are interested in computing the time-dependent coefficients $c_1(t)$ and $c_2(t)$ in order to receive a full solution of the Schroedinger equation. When solving the time-dependent Schroedinger equation, we may employ the solution to the momentum operator in order to simplify the eigensystem associated with $\tilde{\mathbf{H}}$ as follows.

$$i\hbar\partial_t\,|\,\psi\rangle = \mathbf{H}_0|\,\psi\rangle = \frac{\hbar^2}{mR^2}\left(-\frac{1}{2}\left(\frac{\partial}{\partial\tilde{\phi}}\right)^2 \mathbb{1} + \alpha\hat{\mathbf{n}}\boldsymbol{\sigma}\right)|\,\psi\rangle \tag{37}$$

$$= \frac{\hbar^2}{mR^2}\begin{pmatrix} -\frac{1}{2}\left(\frac{\partial}{\partial\tilde{\phi}}\right)^2 + \alpha\cos\tilde{\theta} & \alpha\sin\tilde{\theta}e^{-i\tilde{\phi}} \\ \alpha\sin\tilde{\theta}e^{i\tilde{\phi}} & -\frac{1}{2}\left(\frac{\partial}{\partial\tilde{\phi}}\right)^2 - \alpha\cos\tilde{\theta} \end{pmatrix}|\,\psi\rangle$$

$$= \underbrace{\frac{\hbar^2}{mR^2}\begin{pmatrix} \frac{1}{2}\left(K-\frac{1}{2}\right)^2 + \alpha\cos\tilde{\theta} & \alpha\sin\tilde{\theta}e^{-i\tilde{\phi}} \\ \alpha\sin\tilde{\theta}e^{i\tilde{\phi}} & \frac{1}{2}\left(K+\frac{1}{2}\right)^2 - \alpha\cos\tilde{\theta} \end{pmatrix}}_{\equiv \mathbf{H}_{0,K,\tilde{\phi}}(t)}|\,\psi\rangle \tag{38}$$

where $\tilde{\phi} = \phi - \omega_1 t$ and $\tilde{\theta} = \theta - \omega_2 t$ and where $\mathbf{H}_{0,K,\tilde{\phi}}(t)$ is defined by the last equation.

Setting up the Schroedinger equation for the time-dependent coefficients

Our objective is to set up the Schroedinger equation for the time-dependent coefficients $c_1(t), c_2(t)$, which we do by appropriately transforming the Schroedinger equation for $|\psi\rangle$:

$$i\hbar\partial_t \begin{pmatrix} c_1(t)\psi_1 \\ c_2(t)\psi_2 \end{pmatrix} = \mathbf{H}_0(t) \begin{pmatrix} c_1(t)\psi_1 \\ c_2(t)\psi_2 \end{pmatrix} \tag{39}$$

$$\Leftrightarrow \quad i\hbar\partial_t \begin{pmatrix} c_1(t) \\ c_2(t)\psi_2/\psi_1 \end{pmatrix} = \mathbf{H}_0(t) \begin{pmatrix} c_1(t) \\ c_2(t)\psi_2/\psi_1 \end{pmatrix}$$

Employing the formerly computed solution to the momentum operator, we know that $\psi_2/\psi_1 = e^{i\phi}$ and may write

$$i\hbar\partial_t \begin{pmatrix} c_1(t) \\ c_2(t)e^{i\phi} \end{pmatrix} = \frac{\hbar^2}{mR^2} \begin{pmatrix} \left(\frac{1}{2}(K-\frac{1}{2})^2 + \alpha\cos\tilde{\theta}\right) c_1(t) + \alpha\sin\tilde{\theta}e^{-i\tilde{\phi}}c_2(t)e^{i\phi} \\ \alpha\sin\tilde{\theta}e^{i\tilde{\phi}}c_1(t) + \left(\frac{1}{2}(K+\frac{1}{2})^2 - \alpha\cos\tilde{\theta}\right) c_2(t)e^{i\phi} \end{pmatrix}$$

$$\Leftrightarrow \quad i\hbar\partial_t \begin{pmatrix} c_1(t) \\ c_2(t) \end{pmatrix} = \underbrace{\frac{\hbar^2}{mR^2} \begin{pmatrix} \frac{1}{2}(K-\frac{1}{2})^2 + \alpha\cos\tilde{\theta} & \alpha\sin\tilde{\theta}e^{i\omega_1 t} \\ \alpha\sin\tilde{\theta}e^{-i\omega_1 t} & \frac{1}{2}(K+\frac{1}{2})^2 - \alpha\cos\tilde{\theta} \end{pmatrix}}_{\equiv \mathbf{H}_{0,K,\omega}(t)} \begin{pmatrix} c_1(t) \\ c_2(t) \end{pmatrix} \tag{40}$$

where $\mathbf{H}_{0,K,\omega}(t)$ is defined by the last equation.

Moving into a rotating coordinate system

To solve the eigensystem, we transform $\mathbf{H}_{0,K,\omega}(t)$ by changing into a coordinate system rotating clockwise with a frequency $\omega = \omega_1$:

$$\begin{pmatrix} \tilde{c_1}(t) \\ \tilde{c_2}(t) \end{pmatrix} = e^{-\frac{i}{\hbar}\mathbf{S}_z\omega t} \begin{pmatrix} c_1(t) \\ c_2(t) \end{pmatrix} = e^{-\frac{i}{2}\boldsymbol{\sigma}_z\omega t} \begin{pmatrix} c_1(t) \\ c_2(t) \end{pmatrix} \tag{41}$$

To put it another way, we have

$$\begin{pmatrix} c_1(t) \\ c_2(t) \end{pmatrix} = e^{\frac{i}{2}\boldsymbol{\sigma}_z\omega t} \begin{pmatrix} \tilde{c_1}(t) \\ \tilde{c_2}(t) \end{pmatrix} \tag{42}$$

where

$$e^{\frac{i}{2}\boldsymbol{\sigma}_z\omega t} = \sum_n \frac{\left(\frac{i}{2}\boldsymbol{\sigma}_z\omega t\right)^n}{n!} = \sum_n \frac{\left(\frac{i}{2}\omega t\right)^n}{n!} \begin{pmatrix} 1^n & 0 \\ 0 & (-1)^n \end{pmatrix}$$
$$= \begin{pmatrix} \sum_n \frac{\left(\frac{i}{2}\omega t\right)^n}{n!} & 0 \\ 0 & \sum_n \frac{\left(-\frac{i}{2}\omega t\right)^n}{n!} \end{pmatrix} = \begin{pmatrix} e^{\frac{i}{2}\omega t} & 0 \\ 0 & e^{-\frac{i}{2}\omega t} \end{pmatrix}$$

Implementation of equation (42) in equation (40) gives:

$$i\hbar\partial_t \begin{pmatrix} e^{\frac{i}{2}\omega t} & 0 \\ 0 & e^{-\frac{i}{2}\omega t} \end{pmatrix} \begin{pmatrix} \tilde{c}_1(t) \\ \tilde{c}_2(t) \end{pmatrix} = \mathbf{H}_{0,K,\omega} \begin{pmatrix} e^{\frac{i}{2}\omega t} & 0 \\ 0 & e^{-\frac{i}{2}\omega t} \end{pmatrix} \begin{pmatrix} \tilde{c}_1(t) \\ \tilde{c}_2(t) \end{pmatrix}$$

Transformation of the left-hand side yields:

$$\begin{aligned} e^{-\frac{i}{2}\boldsymbol{\sigma}_z t} \times L.H.S. &= \begin{pmatrix} e^{-\frac{i}{2}\omega t} & 0 \\ 0 & e^{\frac{i}{2}\omega t} \end{pmatrix} \begin{pmatrix} e^{\frac{i}{2}\omega t}\left(-\frac{\hbar\omega}{2} + i\hbar\partial_t\right) & 0 \\ 0 & e^{-\frac{i}{2}\omega t}\left(\frac{\hbar\omega}{2} + i\hbar\partial_t\right) \end{pmatrix} \begin{pmatrix} \tilde{c}_1(t) \\ \tilde{c}_2(t) \end{pmatrix} \\ &= \begin{pmatrix} -\frac{\hbar\omega}{2} & 0 \\ 0 & \frac{\hbar\tilde{\omega}}{2} \end{pmatrix} \begin{pmatrix} \tilde{c}_1(t) \\ \tilde{c}_2(t) \end{pmatrix} + i\hbar\partial_t \begin{pmatrix} \tilde{c}_1(t) \\ \tilde{c}_2(t) \end{pmatrix} \end{aligned}$$

Considering the right-hand side gives:

$$\begin{aligned} e^{-\frac{i}{2}\boldsymbol{\sigma}_z t} \times R.H.S. &= \begin{pmatrix} e^{-\frac{i}{2}\omega t} & 0 \\ 0 & e^{\frac{i}{2}\omega t} \end{pmatrix} \tilde{H}_K \begin{pmatrix} e^{\frac{i}{2}\omega t} & 0 \\ 0 & e^{-\frac{i}{2}\omega t} \end{pmatrix} \begin{pmatrix} \tilde{c}_1(t) \\ \tilde{c}_2(t) \end{pmatrix} \\ &= \begin{pmatrix} \frac{1}{2}(K-\frac{1}{2})^2 + \alpha\cos\tilde{\theta} & \alpha\sin\tilde{\theta} \\ \alpha\sin\tilde{\theta} & \frac{1}{2}(K+\frac{1}{2})^2 - \alpha\cos\tilde{\theta} \end{pmatrix} \begin{pmatrix} \tilde{c}_1(t) \\ \tilde{c}_2(t) \end{pmatrix} \end{aligned}$$

As a consequence, we have

$$i\hbar\partial_t \begin{pmatrix} \tilde{c_1}(t) \\ \tilde{c_2}(t) \end{pmatrix} = \underbrace{\frac{\hbar^2}{mR^2} \begin{pmatrix} \frac{1}{2}(K-\frac{1}{2})^2 + \alpha\cos\tilde{\theta} + \frac{\omega mR^2}{2\hbar} & \alpha\sin\tilde{\theta} \\ \alpha\sin\tilde{\theta} & \frac{1}{2}(K+\frac{1}{2})^2 - \alpha\cos\tilde{\theta} - \frac{\omega mR^2}{2\hbar} \end{pmatrix}}_{\equiv\mathbf{C}} \begin{pmatrix} \tilde{c_1}(t) \\ \tilde{c_2}(t) \end{pmatrix} \tag{43}$$

Comparing equation (43) with the corresponding static Schroedinger equation for time-independent coefficients, one observes that $\mathbf{C}$ is the Hamiltonian one receives when considering a static magnetic field (cf. [18]) combined with an additional matrix $\begin{pmatrix} \frac{\omega mR^2}{2\hbar} & 0 \\ 0 & -\frac{\omega mR^2}{2\hbar} \end{pmatrix}$.

In the following, we will deal with time-independent $\tilde{\theta}$ and time-dependent $\tilde{\phi}$, so that $\tilde{\theta} = \theta = \text{const}$. As eigenvalues of the operator $\mathbf{C}$ we get:

$$E_\pm = \frac{\hbar^2}{mR^2} \left(\frac{K^2 + \frac{1}{4}}{2} \pm \sqrt{\frac{(K - \frac{\omega mR^2}{\hbar})^2}{4} - \alpha(K - \frac{\omega mR^2}{\hbar})\cos\theta + \alpha^2} \right) \tag{44}$$

which correspond to the energies of the lower and the upper band. E_- corresponds to a magnetic moment which is parallel to the magnetic field. As we consider a time-dependent problem, the concept of eigenergies is not applicable without restrictions. In this case, we name the above mentioned eigenvalues eigenenergies as we will find they resurface in the solutions to the initial Schroedinger equation in the form of a dynamic phase factor.

Determining the rotated time-dependent coefficients $\tilde{c}_1(t), \tilde{c}_2(t)$

Our aim now is to determine the solution to equation (43), i.e. find a representation of the rotated time-dependent coefficients $\tilde{c}_1(t), \tilde{c}_2(t)$. An equation of the form

$$i\hbar\partial_t \begin{pmatrix} \tilde{c}_1(t) \\ \tilde{c}_2(t) \end{pmatrix} = \mathbf{C} \begin{pmatrix} \tilde{c}_1(t) \\ \tilde{c}_2(t) \end{pmatrix}$$

can immediately be found to have the solutions

$$\begin{pmatrix} \tilde{c}_{1,+}(t) \\ \tilde{c}_{2,+}(t) \end{pmatrix} = e^{-iE_+t}\mathbf{x}_+ \tag{45}$$

$$\begin{pmatrix} \tilde{c}_{1,-}(t) \\ \tilde{c}_{2,-}(t) \end{pmatrix} = e^{-iE_-t}\mathbf{x}_- \tag{46}$$

where E_+, E_- and $\mathbf{x}_+, \mathbf{x}_-$ are the eigenvalues and the corresponding normalized eigenvectors of the matrix C, respectively. More precisely, the latter are found to be

$$\mathbf{x}_\pm = \begin{pmatrix} x_{1,\pm} \\ x_{2,\pm} \end{pmatrix} = \frac{1}{N_\pm} \begin{pmatrix} \frac{\hbar^2}{mR^2}\left(-\frac{1}{2}(K+\frac{1}{2})^2 + \alpha\cos\theta\right) + \frac{\hbar\omega}{2} + E_\pm \\ \frac{\hbar^2}{mR^2}\alpha\sin\theta \end{pmatrix} \tag{47}$$

with a normalization factor

$$N_\pm^2 = \left(\frac{\hbar^2}{mR^2}\left(-\frac{1}{2}\left(K+\frac{1}{2}\right)^2 + \alpha\cos\theta\right) + \frac{\hbar\omega}{2} + E_\pm\right)^2 + (\alpha\sin\theta)^2 \tag{48}$$

Remark:
This solution for $\tilde{c}_1(t), \tilde{c}_2(t)$ can also be found in a more meticulous way by making use of the matrix $\mathbf{C}$ being diagonalizable. This enables one to write

$$\mathbf{D} = \mathbf{S}^{-1}\mathbf{C}\mathbf{S} = \begin{pmatrix} E_+ & 0 \\ 0 & E_- \end{pmatrix}$$

$$\text{and } \mathbf{C} = \mathbf{S}\mathbf{D}\mathbf{S}^{-1} = \mathbf{S}\begin{pmatrix} E_+ & 0 \\ 0 & E_- \end{pmatrix}\mathbf{S}^{-1}$$

where S is an invertible unitary and time-independent matrix which consists of the column vectors corresponding to the normalized eigenvectors of $\mathbf{C}$. As, with foresight to Section 6, where we discuss the scattering of an incoming wavefunction with energy E_+, we are interested in the solutions to the separate eigenenergies E_+ and E_- rather than a combined solution of both, we consider $\tilde{c}_{i+}(t)$ and $\tilde{c}_{i-}(t)$ separately. Consider $\tilde{c}_{i+}(t)$.

$$\partial_t \begin{pmatrix} \tilde{c}_{1,+}(t) \\ \tilde{c}_{2,+}(t) \end{pmatrix} = \mathbf{S}\begin{pmatrix} E_+/i\hbar & 0 \\ 0 & 0 \end{pmatrix}\mathbf{S}^{-1}\begin{pmatrix} \tilde{c}_{1,+}(t) \\ \tilde{c}_{2,+}(t) \end{pmatrix}$$

$$\Leftrightarrow \mathbf{S}^{-1}\partial_t \begin{pmatrix} \tilde{c}_{1,+}(t) \\ \tilde{c}_{2,+}(t) \end{pmatrix} = \mathbb{1}\begin{pmatrix} E_+/i\hbar & 0 \\ 0 & 0 \end{pmatrix}\mathbf{S}^{-1}\begin{pmatrix} \tilde{c}_{1,+}(t) \\ \tilde{c}_{2,+}(t) \end{pmatrix}$$

Substituting $\mathbf{S}^{-1}\partial_t \begin{pmatrix} \tilde{c}_{1,+}(t) \\ \tilde{c}_{2,+}(t) \end{pmatrix} = \begin{pmatrix} \dot{g}_{1,+}(t) \\ \dot{g}_{2,+}(t) \end{pmatrix}$ we establish a simple system of differential equations

$$\begin{pmatrix} \dot{g}_{1,+}(t) \\ \dot{g}_{2,+}(t) \end{pmatrix} = \begin{pmatrix} E_+/i\hbar & 0 \\ 0 & 0 \end{pmatrix} \begin{pmatrix} g_{1,+}(t) \\ g_{2,+}(t) \end{pmatrix}$$
$$\Longrightarrow \begin{pmatrix} g_{1,+}(t) \\ g_{2,+}(t) \end{pmatrix} = \begin{pmatrix} const. \cdot \; e^{-\frac{i}{\hbar}E_+ t} \\ 0 \end{pmatrix}$$

We now normalize the arbitrary vector and substitute back, i.e. set

$$\begin{pmatrix} \tilde{c}_{1,+}(t) \\ \tilde{c}_{2,+}(t) \end{pmatrix} = \mathbf{S} \begin{pmatrix} g_{1,+}(t) \\ g_{2,+}(t) \end{pmatrix} = \begin{pmatrix} x_{1,+} & x_{1,-} \\ x_{2,+} & x_{2,-} \end{pmatrix} \begin{pmatrix} g_{1,+}(t) \\ g_{2,+}(t) \end{pmatrix} = e^{-\frac{i}{\hbar}E_+ t} \begin{pmatrix} x_{1,+} \\ x_{2,+} \end{pmatrix}$$

In an analogous manner, one finds that

$$\begin{pmatrix} \tilde{c}_{1,-}(t) \\ \tilde{c}_{2,-}(t) \end{pmatrix} = e^{-\frac{i}{\hbar}E_- t} \begin{pmatrix} x_{1,-} \\ x_{2,-} \end{pmatrix}$$

Establishing the solutions to the initial Schroedinger equation, equation (38)

Combining equation (45) and equation (46) with the already computed static parts of the wave function equation (33) and equation (34), as well multiplying the respective components with a factor which sets the wave-function back into a non-rotating coordinate system (see equation (42)), we receive the exact solutions to the initial Schroedinger equation (38).

$$|\psi\rangle_{K,+} = e^{-iE_+ t} \begin{pmatrix} x_{1,+} \; e^{i(K-\frac{1}{2})\phi} \; e^{\frac{i\omega}{2}t} \\ x_{2,+} \; e^{i(K+\frac{1}{2})\phi} \; e^{-\frac{i\omega}{2}t} \end{pmatrix}, \quad {}_{+,K}\langle\psi\,|\,\psi\rangle_{K,+} = 1 \tag{49}$$
$$|\psi\rangle_{K,-} = e^{-iE_- t} \begin{pmatrix} x_{1,-} \; e^{i(K-\frac{1}{2})\phi} \; e^{\frac{i\omega}{2}t} \\ x_{2,-} \; e^{i(K+\frac{1}{2})\phi} \; e^{-\frac{i\omega}{2}t} \end{pmatrix}, \quad {}_{-,K}\langle\psi\,|\,\psi\rangle_{K,-} = 1 \tag{50}$$

These solutions specific to energies E_- and E_+ (and respective bands $+$ and $-$) correspond to solutions to one particular K, hence the indices.

4 Adiabatic Behaviour

4.1 Approximate Solution to $E_\pm$ for $R \to \infty$

In the following, we will determine the approximate solution to $E_\pm$ concerning $\mathbf{H}_0$. As we want to investigate adiabatic behaviour, i.e. a situation where the transition energy between an $\uparrow$-state and $\downarrow$-state is large compared to $\hbar\omega = \hbar\frac{v_F}{R}$, there are two possible limits which can be considered: (a) $\alpha \to \infty$ or (b) $R \to \infty$. The idea is that these correspond to (a) a strong coupling of the spin to the underlying magnetic field leading to a smooth adjustement of the spin or (b) an infinite radius R of the ring, i.e. a magnetic field which changes infinitely slowly.

We consider the case $R \to \infty$ and scale the physical entities accordingly.
K increases linear with R as we require the fermi-energy $E_F = \frac{\hbar^2 k_F^2}{2m}$ to remain the same, i.e. $k_F^2 = \left(\frac{2\pi}{R}n\right)^2, n \in \mathbb{Z}$, should be constant. As the quantum number n is proportional to the momentum K, $n \sim K$, K scales linear with R. α scales quadratically with R, as $\alpha \equiv \frac{\mu_B B_0}{\hbar^2/(mR^2)} \sim R^2$. One expects the rate of change of ϕ, ω, to decrease with increasing adiabacity. We found that under the condition that we scale ω with $\frac{1}{R}$, this produces adiabatic bahaviour of the system.

Thus we scale

$$R \longrightarrow \lambda R, \quad K \longrightarrow \lambda K, \quad \alpha \longrightarrow \lambda^2 \alpha, \quad \omega \longrightarrow \frac{\omega}{\lambda} \tag{51}$$

and consider the limit

$$\lambda \longrightarrow \infty. \tag{52}$$

We will later show that in this limit the system evolves adiabatically by comparing the eigenenergies emerging from the approximation (b) with the eigenenergies determined by the adiabatic ansatz (see Section 4.2).
The exact solution we have established to be

$$E_\pm = \frac{\hbar^2}{mR^2}\left(\frac{K^2+\frac{1}{4}}{2} \pm \sqrt{\frac{(K-\frac{\omega m R^2}{\hbar})^2}{4} - \alpha(K - \frac{\omega m R^2}{\hbar})\cos\theta + \alpha^2}\right)$$

Rescaling according to equation (52) yields

$$\begin{aligned}
E_{\pm,\lambda} =& \frac{\hbar^2}{m\lambda^2R^2}\left(\frac{\lambda^2K^2+\frac{1}{4}}{2} \pm \sqrt{\frac{(\lambda K-\lambda\frac{\omega m R^2}{\hbar})^2}{4} - \lambda^2\alpha\left(\lambda K - \lambda\frac{\omega m R^2}{\hbar}\right)\cos\theta + \lambda^4\alpha^2}\right) \\
=& \frac{\hbar^2}{m\lambda^2R^2}\left(\frac{\lambda^2K^2+\frac{1}{4}}{2} \pm \lambda^2\sqrt{\frac{1}{\lambda^2}\left(\frac{K-\frac{\omega m R^2}{\hbar}}{2}\right)^2 - \frac{\alpha}{\lambda}\left(K - \frac{\omega m R^2}{\hbar}\right)\cos\theta + \alpha^2}\right)
\end{aligned}$$

Next, we Taylor expand the radical term for small $s = \frac{1}{\lambda}$ about $s = 0$. This gives the approximate solution to $E_\pm$ for the above limit $s \to 0$:

$$E_{\pm,s} = \frac{\hbar^2}{mR^2}\left(\frac{K^2}{2} + \alpha + s\left(-\frac{K}{2}\cos\theta + \frac{\omega m R^2}{2\hbar}\cos\theta\right) + \mathbb{O}(s^2)\right) \equiv E_{\pm,lim} \tag{53}$$

Up to first order in s, this solution is independent of the rate of change of ϕ in time, ω.

4.2 Eigenenergies $E_\pm$ Emerging From the Adiabatic Approach

4.2.1 Establishing the Effective Hamiltonian

Our aim is to compare the eigenenergy emerging from an adiabatic ansatz, $E_{\pm,adiab}$, and the exact eigenenergy considered for the limit $R \to \infty$, $E_{\pm,lim}$. If they match, we have convinced ourselves of the fact that the system evolves adiabatically for a large radius $R \to \infty$.

In our set-up, i.e. for a Hamiltonian $\mathbf{H}_0(\mathbf{r}, t) = \frac{\hat{p}^2}{2m_e} + |\mu_B|\mathbf{B}(\mathbf{r}, t) \cdot \boldsymbol{\sigma}$, consider a wave function for an electron at position ϕ in its local ground state (spin in direction of the magnetic field).

Adiabaticity justifies the ansatz

$$|\psi(\phi, t)\rangle = \tilde{\psi}(\phi, t)\,|u(\phi, t)\rangle \tag{54}$$

where $\tilde{\psi}(\phi, t)$ is the amplitude accompanying the ground state $|u(\phi, t)\rangle$ of $\mathbf{H}_0$. Let

$$|u(\phi, t)\rangle = \begin{pmatrix} u_1(\phi, t) \\ u_2(\phi, t) \end{pmatrix} \tag{55}$$

be the spin in the direction of the magnetic field $\mathbf{B}(\phi, t)$.

We will now establish an effective Hamiltonian, expressing the magnetic field in terms of emergent electric and magnetic fields acting on the momentum of the particle.

Projecting the Schroedinger equation onto the local ground state yields:

Left-Hand Side:

$$\begin{aligned}
\langle u(\phi, t)|\, i\hbar\partial_t \left(\tilde{\psi}(\phi, t)\,|u(\phi, t)\rangle\right) &= \langle u(\phi, t)|\left(i\hbar\partial_t\tilde{\psi}(\phi, t)\right)|u(\phi, t)\rangle + \langle u(\phi, t)|\,\tilde{\psi}(\phi, t) i\hbar\partial_t\,|u(\phi, t)\rangle \\
&= i\hbar\partial_t\tilde{\psi}(\phi, t) + i\hbar\tilde{\psi}(\phi, t)\langle u(\phi, t)|\,\partial_t\,|u(\phi, t)\rangle \\
&= \left(i\hbar\partial_t + \Phi_{\text{eff}}(\phi, t)\right)\tilde{\psi}(\phi, t) && (56) \\
\text{where}\quad \Phi_{\text{eff}}(\phi, t) &= i\hbar\langle u|\,\partial_t\,|u\rangle && (57)
\end{aligned}$$

where we have used the shorthand $|u\rangle \equiv |u(\phi, t)\rangle$.

Right-Hand Side:

$$\hat{\mathbf{H}} = \frac{\hat{p}^2}{2m} + \frac{\mu_B g_S}{\hbar}\mathbf{B}(\phi,t)\mathbf{S} = \frac{(-i\hbar\nabla)^2}{2m} + \mu_B \mathbf{B}\boldsymbol{\sigma} = \frac{\hbar^2}{mR^2}\left(-\frac{1}{2}\left(\partial_{\tilde{\phi}}\right)^2 + \alpha\hat{\mathbf{n}}\boldsymbol{\sigma}\right)$$

First, let us consider the kinetic energy.

$$\begin{aligned}
\mathbf{K}\tilde{\psi} =& \langle u|\left(-\frac{\hbar^2}{2mR^2}\left(\partial_\phi\right)^2\tilde{\psi}(\phi,t)\right)|u\rangle = -\frac{\hbar^2}{2mR^2}\langle u|\partial_\phi\left(\partial_\phi\tilde{\psi}|u\rangle + \tilde{\psi}\partial_\phi|u\rangle\right) \\
=& -\frac{\hbar^2}{2mR^2}\left(\langle u|\left((\partial_\phi)^2\tilde{\psi}\right)|u\rangle + 2\cdot\left(\partial_\phi\tilde{\psi}\right)\left(\partial_\phi|u\rangle\right) + \tilde{\psi}(\partial_\phi)^2|u\rangle\right) \\
=& -\frac{\hbar^2}{2mR^2}\left((\partial_\phi)^2\tilde{\psi} + 2\cdot\left(\partial_\phi\tilde{\psi}\right)\langle u|\partial_\phi|u\rangle + \langle u|\tilde{\psi}(\partial_\phi)^2|u\rangle\right)
\end{aligned} \tag{58}$$

Our goal is to rewrite $\mathbf{K}\tilde{\psi}$ as

$$\begin{aligned}
\mathbf{K}\tilde{\psi} =& \left(\frac{(p\mathbb{1} - A_{\text{eff}})^2}{2m} + V_{\text{eff}}\right)\tilde{\psi} \\
=& \left(\frac{p^2}{2m} - \frac{1}{2m}(p\cdot A_{\text{eff}}) - \frac{1}{2m}(A_{\text{eff}}\cdot p) + \frac{A_{\text{eff}}A_{\text{eff}}}{2m} + V_{\text{eff}}\right)\tilde{\psi} \\
& \text{with } A_{\text{eff}} = \frac{i\hbar}{R}\langle u|\partial_\phi|u\rangle \text{ and } V_{\text{eff}} \text{ given below} \qquad (59) \\
=& -\frac{\hbar^2}{2mR^2}\left(\partial_\phi^2\tilde{\psi} + \partial_\phi\langle u|\partial_\phi|u\rangle\tilde{\psi} + \langle u|\partial_\phi|u\rangle\partial_\phi\tilde{\psi} + \underline{|\langle u|\partial_\phi|u\rangle|^2\,\tilde{\psi}}\right) + V_{\text{eff}}\,\tilde{\psi} \qquad (60) \\
& \text{where } \partial_\phi\langle u|\partial_\phi|u\rangle\tilde{\psi} = \underline{\langle\partial_\phi u|\partial_\phi u\rangle}\tilde{\psi} + \langle u|\partial_\phi^2|u\rangle + \langle u|\partial_\phi|u\rangle\partial_\phi\tilde{\psi}
\end{aligned}$$

Comparison of (58) and (60) yields

$$V_{\text{eff}} = \frac{\hbar^2}{2mR^2}\left(\langle\partial_\phi u|\partial_\phi u\rangle - \langle u|\partial_\phi|u\rangle\langle u|\partial_\phi|u\rangle\right) \tag{61}$$

Combining the left- and the right-hand side of the projected Schroedinger equation, we get

$$i\hbar\partial_t\tilde{\psi} = \mathbf{H}_{\text{eff}}\,\tilde{\psi} \quad \text{where } \mathbf{H}_{\text{eff}} = \frac{(p - A_{\text{eff}})^2}{2m} - \Phi_{\text{eff}} + V_{\text{eff}} + \frac{\hbar^2}{2mR^2}\alpha \tag{62}$$

where one would have received a $(-)$ sign in front of the last term if one had chosen a spin directed in the opposite direction with respect to the magnetic field.

As a consequence, comparing the form of the effective vector potential A_{eff} and equation (2), the Berry Phase can be said to manifest itself as a vector potential in the effective Hamiltonian and to induce similar physical properties. The emerging equations of motion also make clear that, when considering the problem from the point of view of the electron, the latter is influenced by a Lorentz force $F_L = -|e|\,(E + \nabla\times A_{\text{eff}})$, with e as the elementary charge and E as the emergent electric field linked to Φ_{eff} and A_{eff}, in addition to a force resulting from the effective potential ($F_{\text{eff}} = -\nabla V_{\text{eff}}$).

Remark:

A common example for a vector potential proving to show physical effects is the Aharanov-Bohm effect, where an isolated magnetic field influences a passing particle as a result of the presence of its vector potential. This influence is observable in the diffraction pattern on the screen, as it is displayed in figure 8.

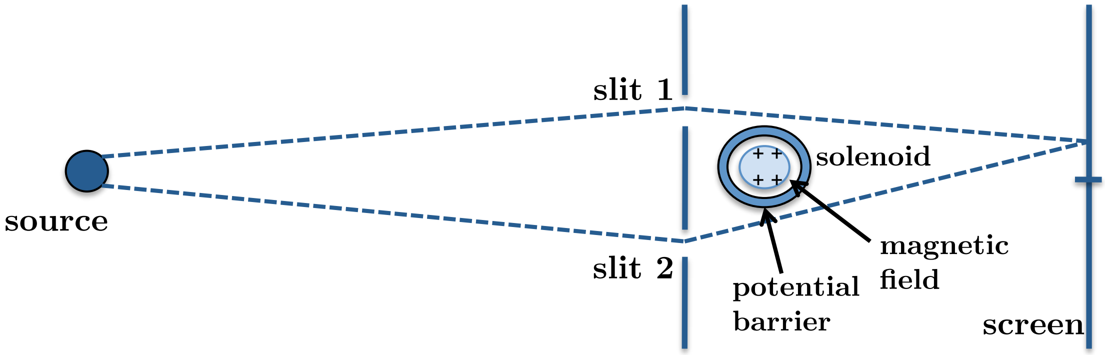

Figure 8: The Aharanov-Bohm effect is the most commonly quoted occurence where the influence of a vector potential on the physics of a wave function is conceivable. Consider a solenoid, i.e. a coil wound up in a helix, with a homogenous and time-independent magnetic field inside the cylinder and isolated with respect to the outside by a potential barrier. Despite the isolation of the interior magnetic field $\mathbf{B} = \nabla \times \ \mathbf{A}$, the presence of the vector potential $\mathbf{A}$ causes a phase-shift in the wave function of the particle. Its effects can be perceived in the diffraction pattern on the screen, compare [22].

4.2.2 Determining the Quantized Energies E_n Corresponding to H_{eff}

Adiabaticity requires that

$$\alpha \hat{\mathbf{n}} \boldsymbol{\sigma} \,|\, u \rangle = \alpha \,|\, u \rangle \tag{63}$$

i.e. the spin should remain locally aligned with respect to the underlying magnetic field at all times. For simplicity reasons, we will restrict ourselves to the case of constant $\tilde{\theta} = \theta$ in the following and vary only $\tilde{\phi}$ in time.

Equation (63) is solved by

$$|\, \hat{u} \rangle = \frac{1}{\sqrt{2 + 2\cos\theta}} \begin{pmatrix} \cos\theta + 1 \\ e^{i\tilde{\phi}} \sin\theta \end{pmatrix} = \begin{pmatrix} e^{-i\tilde{\phi}} \cos\frac{\theta}{2} \\ \sin\frac{\theta}{2} \end{pmatrix} \tag{64}$$

For the purpose of comparing the eigenenergies which are obtained from the different ansatzes, it is essential to rewrite the wave function of the ground state so that it resembles the wave function determined by the exact solution of the Schroedinger equation. It is necessary that the prefactors in the exponents of the exponential functions before the time parameter are the same in the respective vector components. Thus, we redefine

$$|\, u \rangle = \begin{pmatrix} e^{-i\phi} e^{+i\frac{\omega}{2}t} \cos\frac{\theta}{2} \\ e^{-i\frac{\omega}{2}t} \sin\frac{\theta}{2} \end{pmatrix} \tag{65}$$

In order to acquire the complete wave function, we have yet to determine the amplitude $\tilde{\psi}$ of the eigenfunction and therefore construct equation (62).

$$\begin{aligned}
A_{\text{eff}} =& \frac{i\hbar}{R}\langle u|\,\partial_\phi\,|u\rangle = \frac{i\hbar}{R}\begin{pmatrix} e^{i\phi}e^{-i\frac{\omega}{2}t}\cos\frac{\theta}{2} \\ e^{i\frac{\omega}{2}t}\sin\frac{\theta}{2}\end{pmatrix}\begin{pmatrix}(-i)e^{-i\phi}e^{i\frac{\omega}{2}t}\cos\frac{\theta}{2} \\ 0\end{pmatrix} = \frac{\hbar}{R}\cos^2\frac{\theta}{2} \\
\frac{(p-A_{\text{eff}})^2}{2m} =& \frac{1}{2m}\left(-\frac{i\hbar}{R}\partial_\phi - \frac{\hbar}{R}\cos^2\frac{\theta}{2}\right)^2 = \frac{\hbar^2}{2mR^2}\left(-\partial_\phi^2 + 2i\cos^2\frac{\theta}{2}\partial_\phi + \cos^4\frac{\theta}{2}\right) \\
\Phi_{\text{eff}} =& i\hbar\langle u|\,\partial_t\,|u\rangle = i\hbar\begin{pmatrix} e^{i\phi}e^{-i\frac{\omega}{2}t}\cos\frac{\theta}{2} \\ e^{i\frac{\omega}{2}t}\sin\frac{\theta}{2}\end{pmatrix}\begin{pmatrix}(i\frac{\omega}{2})e^{-i\phi}e^{i\frac{\omega}{2}t}\cos\frac{\theta}{2} \\ (-i\frac{\omega}{2})e^{-i\frac{\omega}{2}t}\sin\frac{\theta}{2}\end{pmatrix} \\
=& -\frac{\hbar\omega}{2}\left(\cos^2\frac{\theta}{2} - \sin^2\frac{\theta}{2}\right) = -\frac{\hbar\omega}{2}\cos\theta \\
V_{\text{eff}} =& \frac{\hbar^2}{2mR^2}\left(\langle\partial_\phi u|\,\partial_\phi u\rangle - (\langle u|\,\partial_\phi\,|u\rangle)^2\right) \\
=& \frac{\hbar^2}{2mR^2}\left(\begin{pmatrix} ie^{i\phi}e^{-i\frac{\omega}{2}t}\cos\frac{\theta}{2} \\ 0\end{pmatrix}\begin{pmatrix} -ie^{-i\phi}e^{i\frac{\omega}{2}t}\cos\frac{\theta}{2} \\ 0\end{pmatrix} - \left(\begin{pmatrix} e^{i\phi}e^{-i\frac{\omega}{2}t}\cos\frac{\theta}{2} \\ \sin\frac{\theta}{2}\end{pmatrix}\begin{pmatrix} -ie^{-i\phi}e^{i\frac{\omega}{2}t}\cos\frac{\theta}{2} \\ 0\end{pmatrix}\right)^2\right) \\
=& \frac{\hbar^2}{2mR^2}\left(\cos^2\frac{\theta}{2} + \cos^4\frac{\theta}{2}\right)
\end{aligned}$$

Plugging the expressions above into equation (62) yields the equation

$$\Rightarrow i\hbar\partial_t\tilde{\psi} = \frac{\hbar^2}{2mR^2}\left(\left(-\partial_\phi^2 + 2i\cos^2\frac{\theta}{2}\partial_\phi + 2\cos^4\frac{\theta}{2}\right) + \frac{\omega m R^2}{\hbar}\cos\theta + \cos^2\frac{\theta}{2} + 2\alpha\right)\tilde{\psi} \quad (66)$$

$$\Rightarrow \partial_t\tilde{\psi} = -\frac{i\hbar}{2mR^2}\left(\left(-\partial_\phi^2 + 2i\cos^2\frac{\theta}{2}\partial_\phi + 2\cos^4\frac{\theta}{2}\right) + \frac{\omega m R^2}{\hbar}\cos\theta + \cos^2\frac{\theta}{2} + 2\alpha\right)\tilde{\psi} \quad (67)$$

As we expect $\tilde{\psi}(\phi, t)$ to be a product of an angle-independent and a time-independent function (we have already found the exact solution, which did have this form), we make the product ansatz $\tilde{\psi}(\phi, t) = f(t)g(\phi)$.

$$\Rightarrow \quad \underbrace{\frac{\partial_t f(t)}{f(t)}}_{\equiv -\frac{i}{\hbar}E_n = \text{const.}} = \underbrace{\frac{(a\partial_\phi^2 + b\partial_\phi + c)g(\phi)}{g(\phi)}}_{\equiv -\frac{i}{\hbar}E_n = \text{const.}}$$

We can readily deduce that

$$f(t) = A_1 \cdot e^{-\frac{i}{\hbar}E_n t}, \quad \text{where } A_1 \in \mathbb{C}$$

Making use of the periodic boundary condition $g(\phi) = g(\phi + 2\pi)$, we know that

$$g(\phi) = A_2 \cdot e^{in\phi}, \quad \text{where } A_2 \in \mathbb{C}, n = K - \frac{1}{2} \in \mathbb{Z}$$

As a result, we have

$$\tilde{\psi}(\phi, t) = A \cdot \exp\left(in\phi - \frac{i}{\hbar}E_n t\right), \quad \text{where } A \in \mathbb{C}, n \in \mathbb{Z} \tag{68}$$
$$\text{and } E_n = \frac{\hbar^2}{2mR^2}\left(n^2 - 2n\cos^2\frac{\theta}{2} + 2\cos^4\frac{\theta}{2} + \frac{\omega m R^2}{\hbar}\cos\theta + \cos^2\frac{\theta}{2} + 2\alpha\right)$$

In order to be able to verify that the energy evolving from this strict adiabatic ansatz is in accordance with the approximation for $R \to \infty$ we have made in the previous section, we have to bear in mind that there may be possible shifts in the parameter K. Comparison of the wave functions shows that K is indeed shifted, i.e. $n = K + \frac{1}{2}$. This yields

$$\begin{aligned} E_n &= \frac{\hbar^2}{mR^2}\left(\frac{K^2}{2} + \frac{K}{2} + \frac{1}{8} - \left(K + \frac{1}{2}\right)\cos^2\frac{\theta}{2} + \cos^4\frac{\theta}{2} + \frac{\omega m R^2}{2\hbar}\cos\theta + \frac{1}{2}\cos^2\frac{\theta}{2} + \alpha\right) \\ &= \frac{\hbar^2}{mR^2}\left(\frac{K^2}{2} + \frac{1}{8} - \frac{K}{2}\cos\theta + \cos^4\frac{\theta}{2} + \frac{\omega m R^2}{2\hbar}\cos\theta + \alpha\right) \end{aligned}$$

In order to check if the solution for the adiabtic ansatz is consistent with the exact solution in the limit of $R \to \infty$, we apply the same scaling as in equation (52) so that

$$\begin{aligned} E_n &= \frac{\hbar^2}{m\lambda^2R^2}\left(\frac{\lambda^2K^2}{2} + \frac{1}{8} - \frac{\lambda K}{2}\cos\theta + \cos^4\frac{\theta}{2} + \frac{\lambda\omega m R^2}{2\hbar}\cos\theta + \lambda^2\alpha\right) \\ &= \frac{\hbar^2}{mR^2}\left(\frac{K^2}{2} + \alpha + s\left(-\frac{K}{2}\cos\theta + \frac{\omega m R^2}{2\hbar}\cos\theta\right) + s^2\left(\frac{1}{8} + \cos^4\frac{\theta}{2}\right)\right) \equiv E_{\pm,adiab} \end{aligned} \tag{69}$$

This result is in perfect accordance to linear order in s with equation (53) for a spin in the direction of the magnetic field $\mathbf{B}$. In a similar way, we can show that for a spin antiparallel with respect to $\mathbf{B}$, we achieve equally compatible results.

As the approximate solution for $R \to \infty$ and the one evolving from the adiabatic approach match, we have convinced ourselves that in the limit of $R \to \infty$, our system does indeed behave adiabatically.

5 Berry Phase Physics in a Time-Dependent Magnetic Field

5.1 Determining the Berry Phase

We will now compute the Berry phase of a wave function in our time-dependent magnetic field.

In particular, we should carefully take into account the time dependence of the wave function, which leads to a slightly more complex representation of the phase compared to the case of a static magnetic field. The Berry phase is specific for the parameter space of the Hamiltonian, which in our case is a space-time continuum, so when integrating over a closed loop in parameter space we must not neglect the time component.

In the following, we shall simplify expressions by choosing units such that $\hbar = R = 1$, i.e.

$$\gamma = i \int_0^{2\pi} \langle u(\tilde{\phi}(\phi, t)) \,|\, \partial_{\tilde{\phi}} \,|\, u(\tilde{\phi}(\phi, t)) \rangle d\tilde{\phi} \tag{70}$$

The total differential $d\tilde{\phi}$, where $\tilde{\phi} = \phi - \omega t$, takes the following form:

$$d\tilde{\phi} = \frac{\partial \tilde{\phi}}{\partial \phi} d\phi + \frac{\partial \tilde{\phi}}{\partial t} dt = d\phi - \omega dt \tag{71}$$

Plugging equation (71) into equation (70) above, one has

$$\gamma = i \int_0^{2\pi} \langle u \,|\, \partial_\phi \,|\, u \rangle d\phi - i\omega \int_0^{2\pi/\omega} \langle u \,|\, \partial_\phi \,|\, u \rangle dt \tag{72}$$

For aesthetic purposes, one may consider that

$$\frac{\partial \tilde{\phi}}{\partial t} = -\omega \Rightarrow \frac{\partial}{\partial \tilde{\phi}} = -\frac{1}{\omega} \frac{\partial}{\partial t}$$

and, consequently, one may rewrite equation (72):

$$\gamma = i \int_0^{2\pi} \langle u \,|\, \partial_\phi \,|\, u \rangle d\phi + i \int_0^{2\pi/\omega} \langle u \,|\, \partial_t \,|\, u \rangle dt \tag{73}$$

As a result, we find that the Berry Phase is the sum of the Berry Phase for a time-independent parameter space and an additional part which stems from the extra time parameter.

Spin in Magnetic Field

We consider the particular case of a particle whose spin points in the direction of the externally applied magnetic field, which varies in time. We have already shown that the wave function is given by:

$$|u\rangle_- = \begin{pmatrix} e^{-i\tilde{\phi}} \cos \frac{\theta}{2} \\ \sin \frac{\theta}{2} \end{pmatrix}$$

There are three important limiting cases which may be investigated more closely.

Firstly, consider a static system which is entirely time-independent. In this case, we have $\partial_t \,|\, u\rangle = 0$ and the Berry phase is $\gamma_- = i \int_0^{2\pi} \langle u \,|\, \partial_\phi \,|\, u\rangle d\phi = 2\pi \cos^2 \frac{\theta}{2}$. Alternatively, one may take a different point of view and contemplate the system at a fixed place, $\partial_\phi \,|\, u\rangle = 0$, so that the Berry phase is $\gamma_- = i \int_0^{2\pi/\omega} \langle u \,|\, \partial_t \,|\, u\rangle dt = 2\pi \cos^2 \frac{\theta}{2}$. As expected, both points of view yield the same physical results.

Thirdly, we are interested in a system in which the observer moves with the change of the system so that the motion of the particle and the alteration in the magnetic field cancel each other out exactly, i.e. $-\omega = \frac{2\pi}{T}$. This gives

$$\gamma_- = i \int_0^{2\pi} \langle u \,|\, \partial_\phi \,|\, u\rangle d\phi + i \int_0^{2\pi/\omega} \langle u \,|\, \partial_t \,|\, u\rangle dt = 0 \tag{74}$$

i.e. there would be no change of the wave function.

In an analogous way, we may determine the Berry phase for a spin pointing in the opposite direction, i.e.

$$|u\rangle_+ = \begin{pmatrix} -e^{-i\tilde{\phi}} \sin \frac{\theta}{2} \\ \cos \frac{\theta}{2} \end{pmatrix}. \tag{75}$$

For either of the two first limiting cases we have:

$$\gamma_- = 2\pi \cos^2 \frac{\theta}{2} \tag{76}$$

$$\gamma_+ = 2\pi \sin^2 \frac{\theta}{2} \tag{77}$$

so that $\gamma_- + \gamma_+$ is independent of θ.

5.2 Interpretation of Berry's Phase

We will now investigate possible interpretations of Berry's phase. When introducing the Berry phase, we already discussed the possible geometric analogon of parallel transport, in which the discerning 'phase' is related to the solid angle trespassed on the sphere, see figure 3. We will now follow this thought and examine the relation between the Berry phase and the area trespassed on a sphere.

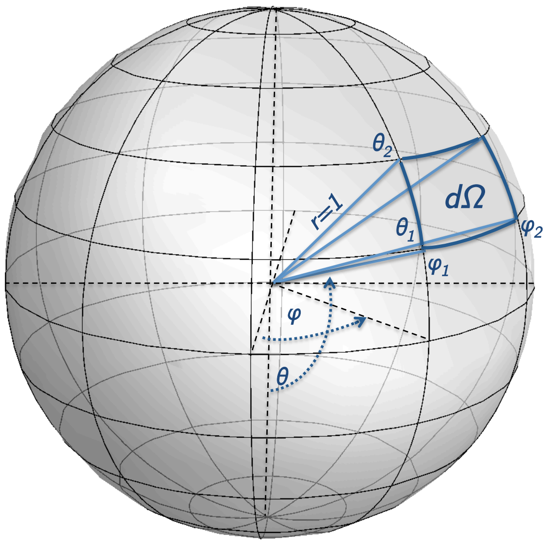

Figure 9: An infinitesimal solid angle is given by $d\Omega = \frac{dA}{r^2} = \sin\theta \; d\theta \; d\phi$. For the infinitesimal area approaching one of the poles, $\sin\theta$ approaches zero, so that the solid angle becomes smaller.

An infinitesimal area on the sphere is given by (see figure 9):

$$dA = (r \sin\theta \; d\theta)(r \; d\phi)$$

and thus the solid angle is

$$d\Omega = \frac{dA}{r^2} = \sin\theta \; d\theta \; d\phi$$

Calculating the solid angle enclosed by the path of the particle is then straightforward:

$$\Omega = \int d\Omega = \int_0^{2\pi} \int_0^{\theta} \sin\theta \; d\phi \; d\theta = 2\pi(1 - \cos\theta) \tag{78}$$

Comparing this result with equation (76) and equation (77), we find that

$$\gamma_- = 2\pi \cos^2 \frac{\theta}{2} = -\frac{\Omega}{2} + 2\pi \tag{79}$$

$$\gamma_+ = 2\pi \sin^2 \frac{\theta}{2} = \frac{\Omega}{2} \tag{80}$$

In effect, considering that $e^{2\pi i} = 1$, we have found $\gamma_\pm = \pm\frac{\Omega}{2}$ which is defined up to mod2π.

We conclude that the Berry phase corresponds to half of the solid angle Ω which is determined by the motion of the particle on the surface of the sphere. The factor two hints at the fact that a spin is only converted into its identity after a rotation of 720° degrees, a rotation about 360° yields a sign. Consequently, after crossing a solid angle of 2π, the Berry phase of a spin-$\frac{1}{2}$-particle is $\pm\pi$ so that $|\,\psi(t=T)\rangle \sim e^{\pm i\pi}\,|\,u\rangle_\pm = -\,|\,u\rangle_\pm$.

Emergent Electrodynamics

We can now compute the effective vector field which arises from the effective vector potential A_{eff}.

$$\mathbf{B}_{\text{eff}} = \text{rot }\mathbf{A} = \nabla \times \left(\frac{\hbar}{R}\cos^2\frac{\theta}{2}\hat{\mathbf{e}}_\phi\right)$$

To evaluate the magnetic field, the physical entity to consider is the magnetic flux density, which proves to be different from zero and which assumes the same form as the Berry phase (for $\hbar = 1$).

$$\begin{aligned}\Phi_{\text{mag}} =& \int_A \mathbf{B}_{\text{eff}}\; d\mathbf{A} = \int_A \nabla \times \mathbf{A}_{\text{eff}}\; dA = \oint_C \mathbf{A}_{\text{eff}}\; ds \\ =& R\int_0^{2\pi} A_\phi\; d\phi = \int_0^{2\pi} \hbar\cos^2\frac{\theta}{2}\; d\phi = 2\pi\hbar\cos^2\frac{\theta}{2}\end{aligned}$$

As a consequence, we may conclude that the physical effect of the Berry phase corresponds to an effective magnetic flux passing through the surface enclosed by the trajectory of the particle with a spin on the ring. The magnetic flux acts on the particle, more specifically it is an orbital magnetic effect, which results from a coupling of the momentum to an effective vector potential. This is opposed to the Zeeman effect, which is related to the coupling of the spin to the orbital momentum.

We are interested in whether the time-dependence of $\tilde{\phi} = \phi - \omega t$ leads to an emergent electric field or not. No such electric field emerges, as

$$E_{\text{eff}} = -\nabla\Phi_{\text{eff}} - \frac{\partial A_{\text{eff}}}{\partial t} = -\partial_\phi \Phi_{\text{eff}} = 0$$

This stems from the fact that the time-dependent problem can be mapped onto a time-independent problem by Galilei-transformations. For this problem we know that there are no emergent electric fields, see also [18]. The Galilean invariance of the problem is further investigated in section 5.3.

However, we expect to find a non-vanishing emergent electric field $E_{\text{eff}} \neq 0$ for time-dependent $\tilde{\theta} = \theta - \omega_2 t$.

5.3 Galilean Invariance

The problem of a time-dependent magnetic field of the form $\mathbf{B} = \mathbf{B}(\tilde{\phi} = \phi - \omega t)$ does not give rise to a substantial change in the physical observables, i.e. no electric field emerges from the time-dependence. This is reflected in the possibility of reversing the time-dependence by a Galilean transformation.

As an example, one may consider a system moving with velocity ω, i.e. producing a translational shift of ϕ corresponding to a transformation back into a time-independent system. For a static system,

$$i\hbar d_t \psi(\phi, t) = i\hbar \partial_t \psi(\phi, t) = \mathbf{H}\psi(\phi, t) \tag{81}$$

For a time-dependent system, we let

$$\psi(\phi, t) \longrightarrow \psi'(\phi', t') = \psi'(\phi - \omega t, t) \tag{82}$$

$$t \longrightarrow t' = t \tag{83}$$

From this transformation one may obtain the Schroedinger equation for the transformed wave function $\psi'(\phi')$.

$$\begin{aligned} i\hbar d_t \psi' =& i\hbar \frac{\partial \psi'}{\partial \phi'} \frac{\partial \phi'}{\partial t} + i\hbar \frac{\partial \psi'}{\partial t} = -i\hbar\omega \frac{\partial \psi'}{\partial \phi'} + i\hbar \frac{\partial \psi'}{\partial t} = \mathbf{H}\psi' \\ \Rightarrow i\hbar \partial_t \psi' =& \left(\mathbf{H} + i\hbar\omega \frac{\partial}{\partial \phi} \mathbb{1} \right) \psi' \end{aligned} \tag{84}$$

Employing the identity

$$\frac{\partial \psi'}{\partial \phi} = \begin{pmatrix} -\psi_1' \cdot \frac{i}{2} \\ \psi_2' \cdot \frac{i}{2} \end{pmatrix}, \tag{85}$$

where ψ_1', ψ_2' are the first and the second components of the wavefunctions $|\psi\rangle_{K,+}$ and $|\psi\rangle_{K,-}$ respectively, we obtain

$$\begin{aligned} i\hbar \partial_t \psi' =& \left(\mathbf{H} + \frac{\hbar\omega}{2} \begin{pmatrix} 1 & 0 \\ 0 & -1 \end{pmatrix} \right) \psi' = \left(\mathbf{H} + \frac{\hbar\omega}{2} \sigma_z \right) \psi' \\ =& \left(\mathbf{H} + \omega S_z \right) \psi' = \mathbf{H}' \psi' \end{aligned} \tag{86}$$

From this we deduce that the problem we consider is Galilean invariant in the way that the Schroedinger equation of the wave function which has undergone a translational shift $-\omega t$ assumes the same form as the static Schroedinger equation. Put differently, the time-dependence of the equation may easily be reversed by a Galilean transformation which leaves the problem invariant.

Alternative: Unitary Transformations

One can also map the time-dependent problem onto a time-independent problem by making use of unitary transformations. We rewrite

$$\begin{aligned}\psi =& \mathbf{U}\tilde{\psi}\\ \mathbf{H} =& \mathbf{U}^{\dagger}\tilde{\mathbf{H}}\mathbf{U}\end{aligned}$$

where $\mathbf{U} = e^{i\frac{\omega}{2}t\boldsymbol{\sigma}_z}$ is a unitary operator, $\mathbf{U}^{\dagger}\mathbf{U} = \mathbb{1}$.
This gives

$$\begin{aligned} & i\hbar\partial_t\psi = \mathbf{H}\psi \\ \Rightarrow & i\hbar\partial_t\mathbf{U}\tilde{\psi} = i\hbar\left(\frac{i\omega}{2}\boldsymbol{\sigma}_z\right)\mathbf{U}\tilde{\psi} + i\hbar\mathbf{U}\partial_t\tilde{\psi} \stackrel{!}{=} \mathbf{H}\mathbf{U}\tilde{\psi} \qquad |\cdot\mathbf{U}^{\dagger} \\ \Leftrightarrow & i\hbar\partial_t\tilde{\psi} = \left(\tilde{\mathbf{H}} + \frac{\hbar\omega}{2}\boldsymbol{\sigma}_z\right)\tilde{\psi}\end{aligned}$$

which yields a simple effective magnetic field in addition to the static Hamiltonian, as before. We may imagine that the spin simply rotates with the time-dependent magnetic field. This situation is not even affected by a static potential scatterer, as the resulting Hamiltonian will still be time-independent. This invariance, however, is not upheld when considering a magnetic impurity as a disturbance in the Hamiltonian.

In the following chapter, we will consider the latter, i.e. the scattering of a spin-$\frac{1}{2}$-particle by a magnetic impurity, which is a problem where the energy is not conserved.

6 Scattering of a Spin-$\frac{1}{2}$-Particle by a Delta-Potential

In the following, we will consider a magnetic impurity as a scatterer of a spin-$\frac{1}{2}$-particle in one dimension. This corresponds for example to a defect in the local magnetic structure inducing a magnetic field, e.g. as a result of strong spin-orbit coupling. From this set-up, we expect to observe spin-flipping scattering processes as well as transitions into other energy bands.

6.1 Turning Back to Eigenenergies

First, let us turn back to the exact eigenenergies we computed in section 3.4, equation (44). We will consider an incoming wave function with a fixed energy

$$E_+ = \frac{\hbar^2}{mR^2}\left(\frac{K^2+\frac{1}{4}}{2} + \sqrt{\frac{(K-\frac{\omega m R^2}{\hbar})^2}{4} - \alpha(K-\frac{\omega m R^2}{\hbar})\cos\theta + \alpha^2}\right) = \text{const.} = \epsilon_0$$

For a fixed energy $\epsilon_n = \epsilon_0 + n\cdot\omega$ there are maximal four real solutions for $K(n,\sigma,\delta)$, which correspond to the propagation directions $\delta = l, r$ and the two possible eigenenergies of the respective wave functions, i.e. the alignment of the spin $\sigma = +,-$ with respect to the magnetic field, see figure 10.

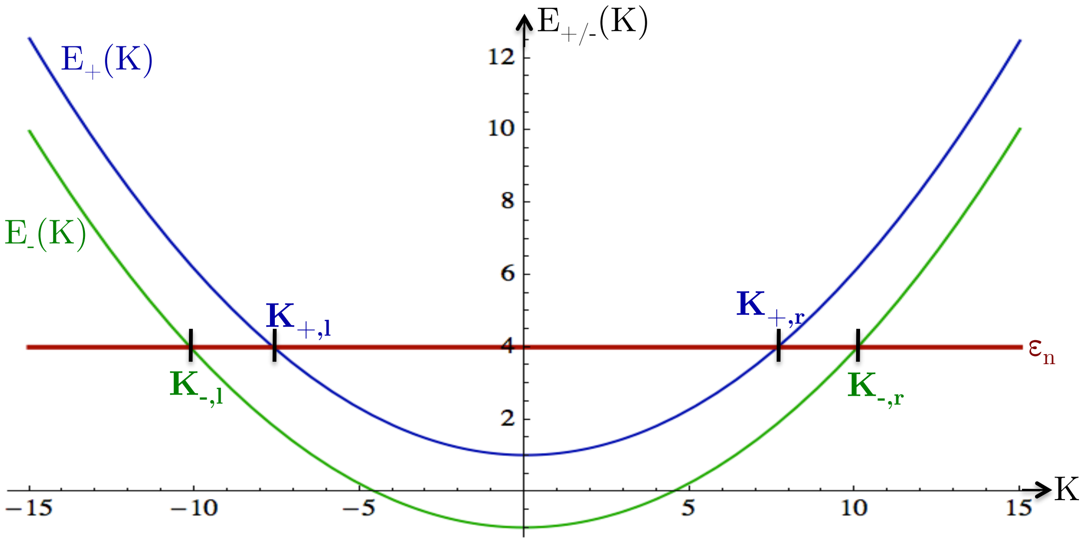

Figure 10: Eigenenergies $E_\pm(K)$ plotted versus the momentum eigenvalue K for sample values of α, ω, θ and $x = \frac{mR^2}{\hbar^2}$. The points of intersection K_i with a fixed energy ϵ determine the propagation direction and the spin alignment of the wave function. We set $\alpha = 10, \quad \omega = 0.1, \quad \theta = \frac{\pi}{2}$ and $x = \frac{mR^2}{\hbar^2} = 10$.

We introduce the notation

$K^n_{+,l}$: wave propagation towards left, spin in direction of magnetic field with energy ϵ_n

$K^n_{+,r}$: wave propagation towards right, spin in direction of magnetic field with energy ϵ_n

$K^n_{-,l}$: wave propagation towards left, spin antiparallel to magnetic field with energy ϵ_n

$K^n_{-,r}$: wave propagation towards right, spin antiparallel to magnetic field with energy ϵ_n

Depending on the energy, there are up to four real solutions for K. The energy function $E_+(K)$ lies below the function $E_-(K)$ for all specific K, see figure 10. For a fixed energy below the minimum of E_- there are no real solutions. For a fixed energy between both minima there are two real solutions which correspond to a spin aligned in the direction of the magnetic field and waves propagating towards the left or the right. For an energy above two minima there are four real solutions. In this case, both directions of propagation and both spin orientations occur.

6.2 Setting Up the Matrix Equation

We consider an impurity in the form of a static delta potential in addition to a magnetic defect, so that

$$\mathbf{H}_1 = \mathbf{H}_0 + (U_0 \mathbb{1} + U_1 \boldsymbol{\sigma}_x)\frac{1}{R}\delta(\phi - \phi_0) \tag{87}$$

where $\mathbf{H}_0$ is the undisturbed Hamiltonian given in equation (6). The prefactor $\frac{1}{R}$ stems from the fact that the delta function has the property that

$$\delta(x) = \begin{cases} 0 & x \neq 0 \\ \infty & x = 0 \end{cases}, \quad \text{and} \quad \int_{-\infty}^{\infty} \delta(x) dx = 1 \tag{88}$$

so that when we create a delta potential at a position s_0, $\delta(s - s_0)$, this corresponds to a delta potential $\frac{1}{R}\delta(\phi - \phi_0)$, as

$$\int_{-\infty}^{\infty} \delta(s - s_0) ds = \int_{-\infty}^{\infty} \delta\left(R(\phi - \phi_0)\right) \frac{1}{R} d\phi = \int_{-\infty}^{\infty} \delta(\phi - \phi_0)\frac{1}{R} d\phi = 1 \tag{89}$$

Our ansatz for solving the Schroedinger equation is motivated by Floquet theory, see [23]. The Floquet theorem states that for a Hamiltonian which is periodic in time, $\mathbf{H}(t) = \mathbf{H}(t+T)$, the solutions to the corresponding Schroedinger equation can be written as $|\,\psi(t)\rangle = \sum_\alpha u_{\alpha,0} e^{-i\epsilon_\alpha t}\,|\,\phi_\alpha(t)\rangle$, where $u_{\alpha,0} = \langle \phi_\alpha(t)\,|\,\psi(0)\rangle$ and α corresponds to the different possible eigenstates (e.g. up, down). $|\,\phi_\alpha(t)\rangle$ can be written, after fourier transformation, as $|\,\phi_\alpha(t)\rangle = \sum_n e^{-in\omega t}\,|\,\phi_{\alpha,n}\rangle$ where $|\,\phi_{\alpha,n}\rangle$ solves the equation

$$(\epsilon_\alpha + n\omega)\,|\,\phi_{\alpha,n}\rangle = \sum_n (\mathbf{H}_F)_{nm}\,|\,\phi_{\alpha,m}\rangle \tag{90}$$

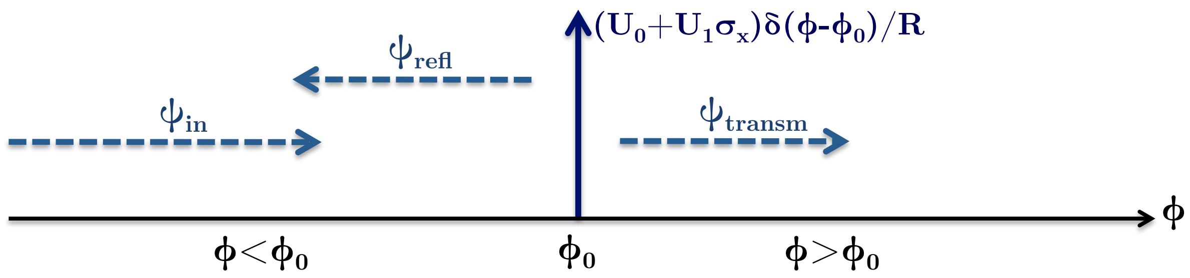

Figure 11: Scattering of a spin-$\frac{1}{2}$-particle by a magnetic impurity: The incoming current density is equal to the sum of the reflected and the transmitted current density.

$\mathbf{H}_F$ is the Floquet Hamiltonian and the $\epsilon_{\alpha,n} = \epsilon_\alpha + n\omega$ define quasienergies up to multiples of $n\omega$, for a full derivation see [24]. In our set-up, we consider an incoming wave function with energy ϵ_0 and allow the incoming particle to gain or lose energy quanta of $\hbar\omega$, so that the resulting (Floquet) state is characterized by its energy $\epsilon_n = \epsilon_0 + n\omega$. Based on this idea, we make the following ansatz for solving the Schroedinger equation $i\hbar\partial_t\boldsymbol{\psi} = \mathbf{H}_1\boldsymbol{\psi}$:

$$\boldsymbol{\chi} = \begin{cases} \boldsymbol{\psi}^0_{+,r} + \sum\limits_{n=-N}^{N}(r^n_{+,l}\boldsymbol{\psi}^n_{+,l} + r^n_{-,l}\boldsymbol{\psi}^n_{-,l}) & : \phi < \phi_0 \\ \sum\limits_{n=-N}^{N}(t^n_{+,r}\boldsymbol{\psi}^n_{+,r} + t^n_{-,r}\boldsymbol{\psi}^n_{-,r}) & : \phi > \phi_0 \end{cases} \tag{91}$$

Consequently, we make the ansatz that the wave function on the left hand side and the right hand side are given by sums of wave functions with energies $\epsilon_n = \epsilon_0 + n\omega$, with amplitudes $r^n_{\sigma,\delta}, t^n_{\sigma,\delta}$ which correspond to reflection and transmission coefficients, respectively. A boundary (leap) condition is imposed by the delta-potential. When integrating

$$i\hbar\partial_t\boldsymbol{\chi} = \frac{\hbar^2}{mR^2}\left(-\frac{1}{2}\left(\frac{\partial}{\partial\tilde{\phi}}\right)^2\mathbb{1} + \alpha\hat{\mathbf{n}}\boldsymbol{\sigma} + \frac{mR}{\hbar^2}(U_0 + U_1\boldsymbol{\sigma}_x)\delta(\phi - \phi_0)\right)\boldsymbol{\chi} \tag{92}$$

over an ϵ-environment around ϕ_0 and using

$$\int_{\pi-\epsilon}^{\pi+\epsilon}\frac{\partial^2}{\partial\phi^2}\boldsymbol{\chi}(\phi,t)d\phi = \boldsymbol{\chi}'(\pi+\epsilon,t) - \boldsymbol{\chi}'(\pi-\epsilon,t).$$

integration yields

$$-\frac{1}{2}\left(\boldsymbol{\chi}'(\pi+\epsilon) - \boldsymbol{\chi}'(\pi-\epsilon,t)\right) + \alpha\hat{\mathbf{n}}\boldsymbol{\sigma}\underbrace{\int_{\pi-\epsilon}^{\pi+\epsilon}\boldsymbol{\chi}(\phi,t)d\phi}_{\sim\mathbb{O}(\epsilon)} + \frac{mR}{\hbar^2}(U_0+U_1\boldsymbol{\sigma}_x) = \frac{imR^2}{\hbar}\partial_t\underbrace{\int_{\pi-\epsilon}^{\pi+\epsilon}\boldsymbol{\chi}(\phi,t)d\phi}_{\sim\mathbb{O}(\epsilon)}$$

From the limit $\epsilon \longrightarrow 0$ follows the first boundary condition

$$\boldsymbol{\chi}'(\phi_0^+) - \boldsymbol{\chi}'(\phi_0^-) = \frac{2mR}{\hbar^2}(U_0 + U_1\boldsymbol{\sigma}_x)\boldsymbol{\chi}(\phi_0,t) \tag{93}$$

The renewed integration of equation (92) leads to a second condition, demanding continuity of the wave function at ϕ_0, i.e.

$$\boldsymbol{\chi}(\phi_0^+) = \boldsymbol{\chi}(\phi_0^-) \tag{94}$$

We can determine the reflection and transmission coefficients by setting up a matrix equation $\mathbf{M} \cdot \mathbf{a} = \mathbf{b}$, where $\mathbf{a}$ is a vector with $4(2N+1)$ entries and made up of reflection and transmission coefficients for different energies ϵ_n and $\mathbf{M}$, $\mathbf{b}$ are determined by the boundary conditions. The matrix $\mathbf{M}$ is made up of submatrices $\mathbf{M}_0^n, \mathbf{M}_1^n, \mathbf{M}_2^n$ sized (4×4) corresponding to one particular n. Consequently, $\mathbf{M}$ is a $(4(2N+1) \times 4(2N+1))$-matrix. We receive

$$\sum_{n=-N}^{N} \mathbf{M}^n \mathbf{a}^n = \sum_{n=-N}^{N} \left(\mathbf{M}_0^n e^{-in\omega t} + \mathbf{M}_1^n e^{-i(n+1)\omega t} + \mathbf{M}_2^n e^{-i(n-1)\omega t} \right) \mathbf{a}^n = \mathbf{b}^0 \tag{95}$$

where indices n stand for respective energies ϵ_n of the wave function.

The (4×4)-submatrices for specific n are given by

$$\mathbf{M}_0^n = (\mathbf{m}_{0,1}^n, \mathbf{m}_{0,2}^n, \mathbf{m}_{0,3}^n, \mathbf{m}_{0,4}^n)^T$$

where

$$\mathbf{m}_{0,1}^n = \left(-\mathbf{x}_{1,+,l}^n e^{iK_{+,l}^n \phi_0},\ -\mathbf{x}_{1,-,l}^n e^{iK_{-,l}^n \phi_0},\ \mathbf{x}_{1,+,r}^n e^{iK_{+,r}^n \phi_0},\ \mathbf{x}_{1,-,r}^n e^{iK_{-,r}^n \phi_0} \right)$$

$$\mathbf{m}_{0,2}^n = \left(-\mathbf{x}_{2,+,l}^n e^{iK_{+,l}^n \phi_0},\ -\mathbf{x}_{2,-,l}^n e^{iK_{-,l}^n \phi_0},\ \mathbf{x}_{2,+,r}^n e^{iK_{+,r}^n \phi_0},\ \mathbf{x}_{2,-,r}^n e^{iK_{-,r}^n \phi_0} \right)$$

$$\begin{aligned}\mathbf{m}_{0,3}^n = \Bigg(& -i(K_{+,l}^n - \frac{1}{2})\ \mathbf{x}_{1,+,l}^n e^{iK_{+,l}^n \phi_0},\ -i(K_{-,l}^n - \frac{1}{2})\ \mathbf{x}_{1,-,l}^n e^{iK_{-,l}^n \phi_0}\ , \\ & \left(i(K_{+,r}^n - \frac{1}{2}) - \frac{2mR}{\hbar^2} U_0 \right) \mathbf{x}_{1,+,r}^n e^{iK_{+,r}^n \phi_0},\ \left(i(K_{-,r}^n - \frac{1}{2}) - \frac{2mR}{\hbar^2} U_0 \right) \mathbf{x}_{1,-,r}^n e^{iK_{-,r}^n \phi_0} \Bigg)\end{aligned}$$

$$\begin{aligned}\mathbf{m}_{0,4}^n = \Bigg(& -i(K_{+,l}^n + \frac{1}{2})\ \mathbf{x}_{2,+,l}^n e^{iK_{+,l}^n \phi_0},\ -i(K_{-,l}^n + \frac{1}{2})\ \mathbf{x}_{2,-,l}^n e^{iK_{-,l}^n \phi_0}\ , \\ & \left(i(K_{+,r}^n + \frac{1}{2}) - \frac{2mR}{\hbar^2} U_0 \right) \mathbf{x}_{2,+,r}^n e^{iK_{+,r}^n \phi_0},\ \left(i(K_{-,r}^n + \frac{1}{2}) - \frac{2mR}{\hbar^2} U_0 \right) \mathbf{x}_{2,-,r}^n e^{iK_{-,r}^n \phi_0} \Bigg)\end{aligned}$$

and

$$\mathbf{M}_1^n = \begin{pmatrix} 0 & 0 & 0 & 0 \\ 0 & 0 & 0 & 0 \\ 0 & 0 & -\frac{2mR}{\hbar^2} U_1 \mathbf{x}_{2,+,r}^n e^{iK_{+,r}^n \phi_0} e^{i\phi_0} & -\frac{2mR}{\hbar^2} U_1 \mathbf{x}_{2,-,r}^n e^{iK_{-,r}^n \phi_0} e^{i\phi_0} \\ 0 & 0 & 0 & 0 \end{pmatrix}$$

$$\mathbf{M}_2^n = \begin{pmatrix} 0 & 0 & 0 & 0 \\ 0 & 0 & 0 & 0 \\ 0 & 0 & 0 & 0 \\ 0 & 0 & -\frac{2mR}{\hbar^2} U_1 \mathbf{x}_{1,+,r}^n e^{iK_{+,r}^n \phi_0} e^{-i\phi_0} & -\frac{2mR}{\hbar^2} U_1 \mathbf{x}_{1,-,r}^n e^{iK_{-,r}^n \phi_0} e^{-i\phi_0} \end{pmatrix}$$

$\mathbf{M}_0^n$ is the matrix which is characteristic of the static delta potential, $\mathbf{M}_1^n, \mathbf{M}_2^n$ represent off-diagonal terms produced by the magnetic impurity. The vector of coefficients $\mathbf{a}^n$ and the inhomogenous vector $\mathbf{b}^n$ are given by

$$\mathbf{a}^n = \begin{pmatrix} r_{+,l}^n \\ r_{-,l}^n \\ t_{+,r}^n \\ t_{-,r}^n \end{pmatrix}, \quad \mathbf{b}^n = \delta_{m,0} \begin{pmatrix} \mathbf{x}_{1,+,r}^m e^{iK_{+,r}^m \phi_0} \\ \mathbf{x}_{2,+,r}^m e^{iK_{+,r}^m \phi_0} \\ i(K_{+,r}^m - \frac{1}{2})\mathbf{x}_{1,+,r}^m e^{iK_{+,r}^m \phi_0} \\ i(K_{+,r}^m + \frac{1}{2})\mathbf{x}_{2,+,r}^m e^{iK_{+,r}^m \phi_0} \end{pmatrix}$$

In order to cancel out the sum in the matrix problem, we integrate equation (95) over time and consider the general matrix elements

$$\mathbf{A}_{mn} = \int dt e^{im\omega t} \mathbf{A}^n = \int dt e^{im\omega t} (\mathbf{M}_0^n e^{-in\omega t} + \mathbf{M}_1^n e^{-i(n+1)\omega t} + \mathbf{M}_2^n e^{-i(n-1)\omega t}) \tag{96}$$

$$= 2\pi(\mathbf{M}_0^n \delta_{m,n} + \mathbf{M}_1^n \delta_{m,n+1} + \mathbf{M}_2^n \delta_{m,n-1}) \tag{97}$$

$$\text{and} \tag{98}$$

$$\int_{-\infty}^{\infty} dt \mathbf{b}^m \delta_{m0} e^{im\omega t} = 2\pi\delta(m\omega)\mathbf{b}^m \delta_{m0} = 2\pi \mathbf{b}^m \delta_{m0} \tag{99}$$

where we have used the identity

$$\delta(x-\alpha) = \frac{1}{2\pi} \int_{-\infty}^{\infty} e^{ip(x-\alpha)} dp \tag{100}$$

From the form of the general matrix elements it becomes clear that, resulting from the shift in exponents by $\pm i\omega t$, secondary diagonal terms emerge in the form of submatrices $\mathbf{M}_1^n, \mathbf{M}_2^n$.

The resulting matrix equation takes the following form:

$$\begin{pmatrix} \mathbf{M}_0^{-N} & \mathbf{M}_2^{-N} & 0 & & \cdots & & & 0 \\ \mathbf{M}_1^{-N+1} & \mathbf{M}_0^{-N+1} & \mathbf{M}_2^{-N+1} & 0 & & & & \\ 0 & & & & & & & \vdots \\ & & & & \ddots & & & \\ \vdots & & & & & & & 0 \\ & & & & 0 & \mathbf{M}_1^{N-1} & \mathbf{M}_0^{N-1} & \mathbf{M}_2^{N-1} \\ 0 & & \cdots & & & 0 & \mathbf{M}_1^N & \mathbf{M}_0^N \end{pmatrix} \cdot \begin{pmatrix} \mathbf{a}^{-N} \\ \vdots \\ \mathbf{a}^0 \\ \vdots \\ \mathbf{a}^N \end{pmatrix} = \begin{pmatrix} 0 \\ \vdots \\ 0 \\ \mathbf{b}^0 \\ 0 \\ \vdots \\ 0 \end{pmatrix} \tag{101}$$

The off-diagonal terms are indicative of transitions into other energy bands and are characteristic of the magnetic impurity, as it is clear that they vanish for $U_1 = 0$.

What is more, we expect these off-diagonal terms to decrease with increasing energy $E + n \cdot \omega$, so that energy transitions into states with ϵ_0 plus large multiples of $\hbar\omega$ are less likely.

As a result, we are able to neglect off-diagonal terms for certain $|n| > n_0$. From a technical point of view, this increasing suppression of matrix entries for growing n becomes apparent when considering that the K_i increase with higher energies.

We find numerically that physical entities only marginally deviate from each other for different N as early as for $N > N_0 = 2$. This is why, to allow for a greater range in values ω, in Section 6.4, most plots have been computed for $N = 2$.

6.3 Physical Entity Conserved in the Scattering Process

To determine the physical entity conserved in the scattering process, we consider the continuity equation of quantum mechanics

$$\nabla \cdot \mathbf{j} = -\partial_t \rho = 0 \tag{102}$$

where $\mathbf{j}$ is the probability current and $\rho = |\boldsymbol{\psi}|^2$ is the probability density function.

With the objective of determining the exact form of the probability current $\mathbf{j}$, consider the time-dependent Schroedinger equation for $\boldsymbol{\psi}$ and its hermitian conjugate.

$$\begin{aligned} i\hbar\partial_t \boldsymbol{\psi} &= -\frac{\hbar^2}{2m}\frac{\partial^2 \boldsymbol{\psi}}{\partial x^2} - \mu_B B_0 \hat{\mathbf{n}}\boldsymbol{\sigma}\boldsymbol{\psi} \\ -i\hbar\partial_t \boldsymbol{\psi}^* &= -\frac{\hbar^2}{2m}\frac{\partial^2 \boldsymbol{\psi}^*}{\partial x^2} - \mu_B B_0 \hat{\mathbf{n}}\boldsymbol{\sigma}\boldsymbol{\psi}^* \end{aligned}$$

Subtraction yields:

$$i\hbar\partial_t(\boldsymbol{\psi}^*\boldsymbol{\psi}) = i\hbar\partial_t |\boldsymbol{\psi}|^2 \stackrel{!}{=} -\frac{\hbar^2}{2m}(\boldsymbol{\psi}^*\partial_x^2\boldsymbol{\psi} - \boldsymbol{\psi}\partial_x^2\boldsymbol{\psi}^*)$$

Using equation 102, we may write

$$\nabla \cdot \mathbf{j} = \frac{\hbar}{2mi}(\boldsymbol{\psi}^*\partial_x^2\boldsymbol{\psi} - \boldsymbol{\psi}\partial_x^2\boldsymbol{\psi}^*)$$

and from this follows

$$\mathbf{j} = \frac{\hbar}{2mi}(\boldsymbol{\psi}^*\boldsymbol{\psi}' - \boldsymbol{\psi}\boldsymbol{\psi}^{*'}) = \frac{\hbar}{m}\Im(\boldsymbol{\psi}^*\boldsymbol{\psi}') \tag{103}$$

We numerically reviewed that the current for a specific wavefunction $\boldsymbol{\psi}(K, n)$ is equal to the amplitude of the wavefunction multiplied with the derivative of the energy by k evaluated for the respective K, n.

$$\mathbf{j}_{K_{\sigma,\delta}} = \frac{\hbar}{m}\Im(\boldsymbol{\psi}^*_{\sigma,\delta}\boldsymbol{\psi}'_{\sigma,\delta}) = \frac{\hbar}{m}\boldsymbol{\psi}^*_{\sigma,\delta}\left[\frac{\partial E}{\partial K}\right]_{K_{\sigma,\delta}}\boldsymbol{\psi}_{\sigma,\delta} \tag{104}$$

where $\sigma = +, -$ and $\delta = l, r$.

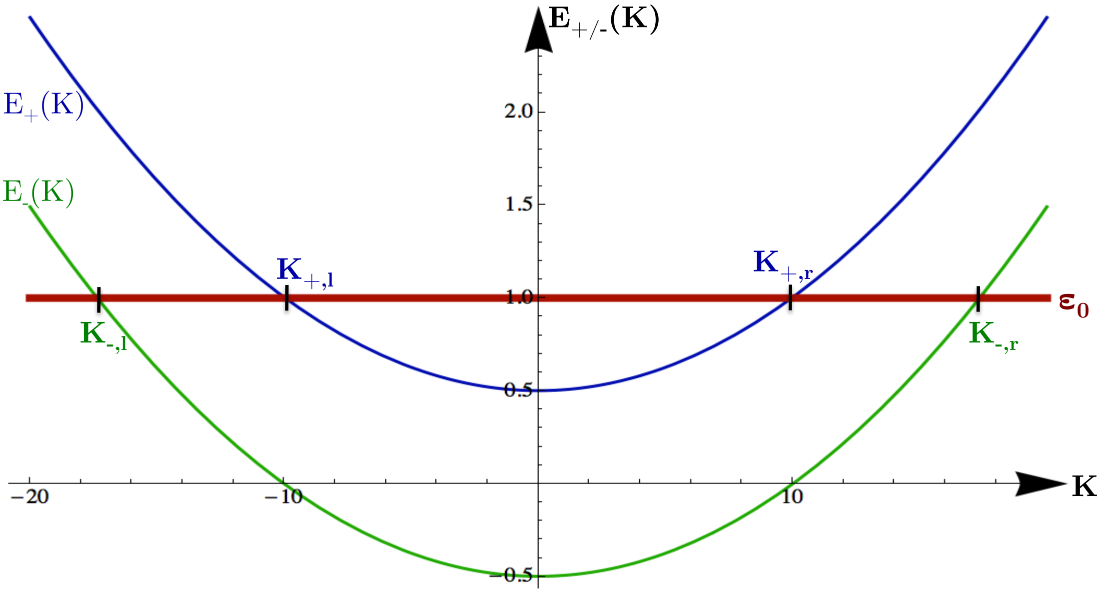

Figure 12: Eigenenergies $E_{\pm}(K)$ plotted versus the momentum eigenvalue K for fixed values of $\mu_B B, \omega, \theta$ and $x = R^2$ and possible points of intersection K_i with the energy of the incoming wave-function $\epsilon_0 = 1$. The points of intersection K_i with a fixed energy ϵ determine the propagation direction and the spin alignment of the wave function. We set $\mu_B B_0 = 0.5$, $\omega \to 0$, $\theta = \frac{\pi}{2}$ and $x = R^2 = 100$.

Taking into account the direction of motion of the waves, the law of conservation is

$$\mathbf{j}_{in} = -\,\mathbf{j}_{\text{refl.}} + \mathbf{j}_{\text{transm.}} \tag{105}$$

$$\Rightarrow \frac{\partial E^0_{+r}}{\partial K} = \sum_n \left\{ -\left(|r^n_{+l}| \left[\frac{\partial E}{\partial K}\right]^n_{+l} + |r^n_{-l}| \left[\frac{\partial E}{\partial K}\right]^n_{-l} \right) + \left(|t^n_{+r}| \left[\frac{\partial E}{\partial K}\right]^n_{+r} + |t^n_{-r}| \left[\frac{\partial E}{\partial K}\right]^n_{-r} \right) \right\},$$

which we have also confirmed numerically.

6.4 The Spin-Flip-Rate

In the following, we set $m = \hbar = 1$ and consider an incoming wave function with energy $\epsilon_0 = 1$. We will scale all other parameters accordingly, using physical units where not specified otherwise. We are interested only in a regime where there are 4 real solutions K^n to the equations $E_{\pm} = \epsilon_0 + n\omega$, i.e. where the energy $\epsilon_n = \epsilon_0 + n\omega$ lies above the minimum of $E_+(K)$. Put differently, this corresponds to a system where $N \cdot \omega$ (with N the maximum quantum number) is smaller than the distance between ϵ_0 and the minimum of $E_+(K)$, see figure 12. As an example, for $N = 2$ the possible range of ω is limited to approximately $-0.24 < \omega < 0.24$. We will also be choosing $\mu_B B_0 < \epsilon_0$ since the energy gap, when Taylor expanded around $\mu_B B_0 = 0$ in first order of $\mu_B B_0$, is proportional to $2\cos\theta\mu_B B_0$. From

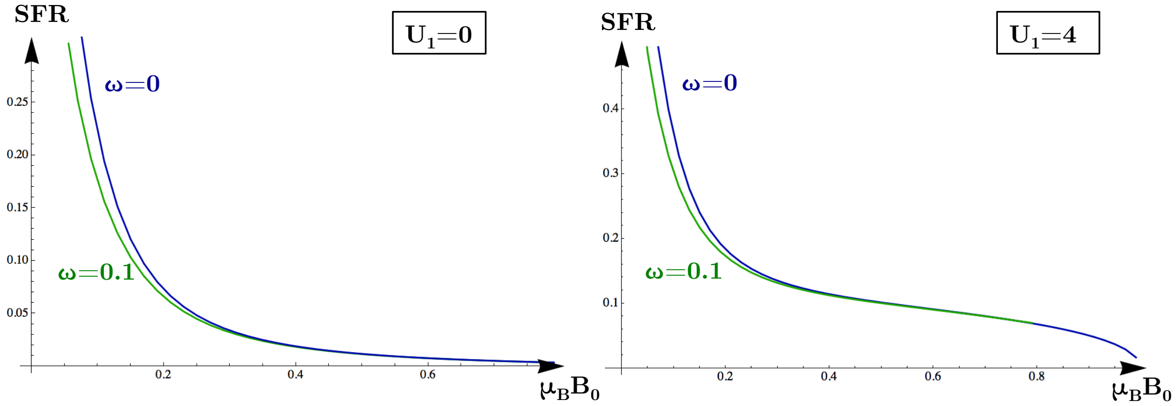

Figure 13: The plot shows the spin-flip-rate (SFR) as a function of the amplitude of the underlying magnetic field, $\mu_B B_0$. As the coupling between the spin of the electron and the magnetization grows stronger, the spin-flip-rate increases, approaching zero for $\mu_B B_0 \approx \epsilon_F$. The blue curve represents the case of a frequency $\omega \to 0$, the green curve has been computed for $\omega = 0.1$. A magnetic impurity with an amplitude different from zero induces additional spin-flipping (see right hand side of the figure). We also chose $\phi_0 = 0$, $\theta = \pi/2$, $x = R^2 = 100$, $U_0 = 2$.

a physical point of view, for large $\mu_B B_0$, the spin couples more strongly to the magnetic structure and is thus less likely to flip. Since we want to find transitions to other spin states and in order to allow for more discrete energy levels above the minimum of E_+, we choose $\mu_B B_0$ small compared to the fermi energy. The dependence of the spin-flip-rate on $\mu_B B_0$ is displayed in figure 13.

Particular emphasis will be put on the case of a large radius R, as this is the adiabatic case, which is why in general we will set $R = 10$.

In this section, we will further investigate the behaviour of the spin when meeting a magnetic potential barrier in the form of a delta potential. We define the spin-flip-rate as the current induced by all reflected and transmitted waves where the spin is 'up' (previously denoted as '-'), divided by the current induced by the incoming wave (with spin down).

$$SFR \equiv \frac{\sum_n \left\{ -\left(|r^n_{-l}| \left[\frac{\partial E}{\partial K}\right]^n_{-l} \right) + \left(|t^n_{-r}| \left[\frac{\partial E}{\partial K}\right]^n_{-r} \right) \right\}}{j_{in}} \tag{106}$$

When plotting the spin-flip-rate against the radius of the ring, see figure 14, adiabatic characteristics are observable in the form of a rapid decrease in the spin-flip-rate for growing R. When the magnetic structure becomes smoother (adiabatic limit), the local magnetic order is approximately ferromagnetic and the spin becomes less likely to flip. In the limit of R to infinity, no quantum mechanical phase is acquired and the coupling of the spin to the magnetic structure is at its maximum.

We are also interested in how the spin-flip-rate changes for different choices of the amplitudes of the impurities. For both static and magnetic impurities we observe a strong peak in the spin-flip-rate which corresponds to one particular potential amplitude of order ϵ_F, see figure 15. Apparently, for a magnetic potential barrier which is about as high as the non-magnetic potential barrier, spins are most likely to flip. For potentials higher than the fermi energy, the spin flip rate decreases dramatically and above a value of approximately 20, it stays nearly constant.

When plotting the rate of transmission against the various potentials, one observes total reflection for $U_0, U_1 > 20$: for this height of the potential barrier, which is of far greater magnitude than ϵ_0, the probability of tunneling vanishes, as one expects.

A distinctive curve emerges when the dependence of the spin-flip-rate on the frequency ω is plotted, see figure 16. The first observation one makes is that for large $\mu_B B_0$ (one magnitude smaller than the fermi-energy), the spin-flip-rate stays approximately constant, whereas for smaller magnetic fields the spin-flip-rate assumes a maximum for values of ω near zero. For very small magnetic fields the form of the curve resembles a box.

For all magnetic fields, the spin-flip-rate is independent of ω for $|\omega|$ larger than a certain value $|\omega_0|$. When crossing a certain frequency, however, the spin-flip-rate increases (smoothly for large magnetic fields, more abruptly for very small magnetic fields) to an astonishingly high value of 0.8, and then rests upon a higher plateau of a nearly constant spin-flip-rate for a whole region of $|\omega|<|\omega_0|$. For small magnetic fields and rotation frequencies ω near zero, the excitation rate of the spin into another spin state is particularly high.

The width of the peak depends on the choice of the radius R. For increasing R, the width of the box w decreases, however the respective heights of the plateaus stay the same, see figure 18. The proportionality of the width of the box w and the radius R is linear, $w \sim R^{-1}$, see figure 19. This hints at the fact that high rates of spin-flip are confined to smaller regions of ω for increasing adiabaticity, i.e. for nearly ferromagnetic structures. The box width is given by the fermi velocity v_F. For $\omega R = v_F$, the rim of the box is reached and the spin-flip-rate decreases rapidly, reaching its new lower level. This is in accordance with the adiabatic limit that v_F/R is small compared to the splitting frequency.

One also observes two peaks at both ends of the box for small magnetic fields. These are particularly distinct when considering very small magnetic fields approaching zero (anti-adiabatic limit), when the coupling to the magnetic field vanishes. They result from effects caused by the magnetic impurity, which becomes clear when considering figure 17. Their difference in height and thus the break in symmetry of the spin-flip-rate may be the consequence of our choice of an incoming wave propagating to the right.

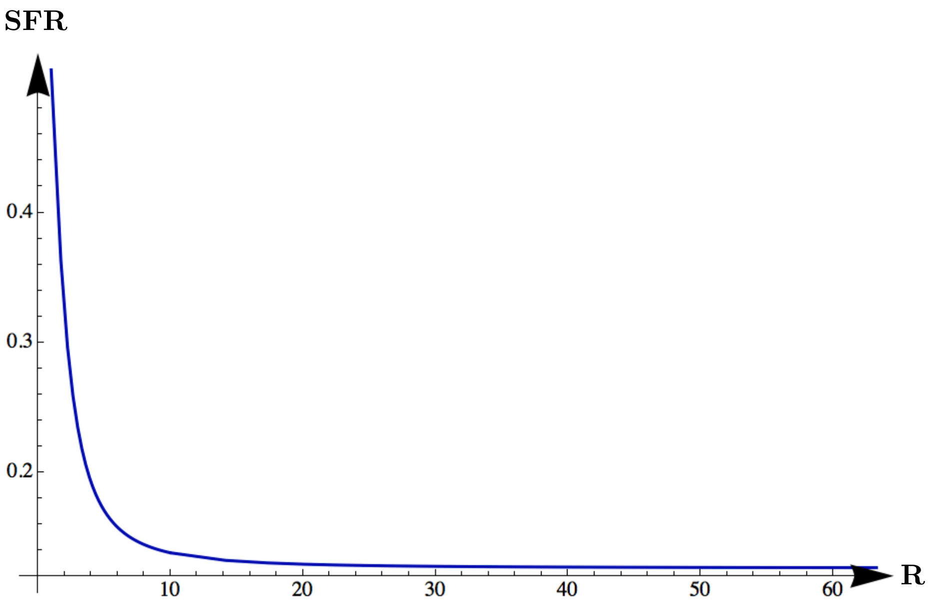

Figure 14: The plot shows the spin-flip-rate (SFR) as a function of R (large R correspond to a slow change of the magnetic structure). When the magnetic structure becomes smoother (adiabatic limit), the local magnetic order is approximately ferromagnetic and the spin becomes less likely to flip. We chose $\mu_B B_0 = 0.5,\ \phi_0 = 0,\ \theta = \pi/2,\ U_0 = 2,\ U_1 = 4$.

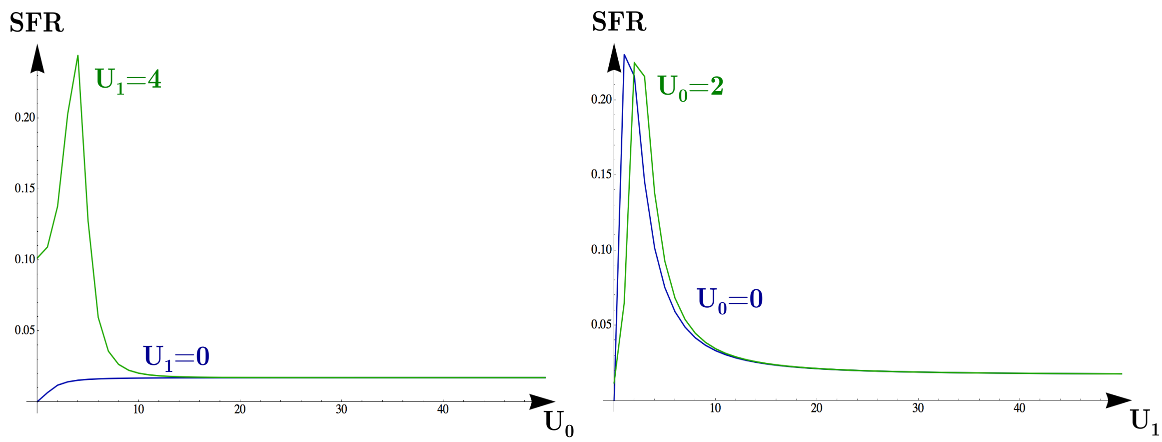

Figure 15: The plot shows the spin-flip-rate (SFR) as a function of the amplitudes of the static and magnetic impurities U_0, U_1. The green curves represent systems where both static and magnetic impurities are present with given non-zero amplitudes, whereas the blue curves show the spin-flip-rate for purely static and magnetic impurities, respectively. We chose $\mu_B B_0 = 0.5,\ \phi_0 = 0,\ x = R^2 = 100,\ \theta = \pi/2$.

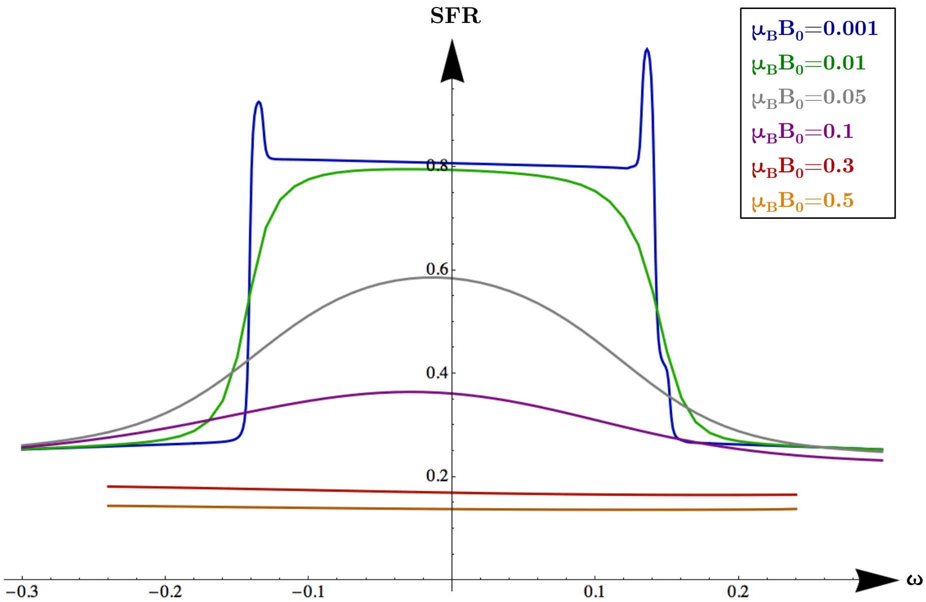

Figure 16: The plot shows the spin-flip-rate (SFR) as a function of the frequency ω with which the underlying magnetic field varies in time. The SFR remains constant and indifferent to the frequency for $|\ \omega\ |> 0.15$. For small magnetic fields and rotation frequencies ω near zero, the excitation rate of the spin into another spin state is particularly high. We chose $\mu_B B_0$ as given in the figure and also set $\phi_0 = 0,\ x = R^2 = 100,\ \theta = \pi/2,\ U_0 = 2,\ U_1 = 4$.

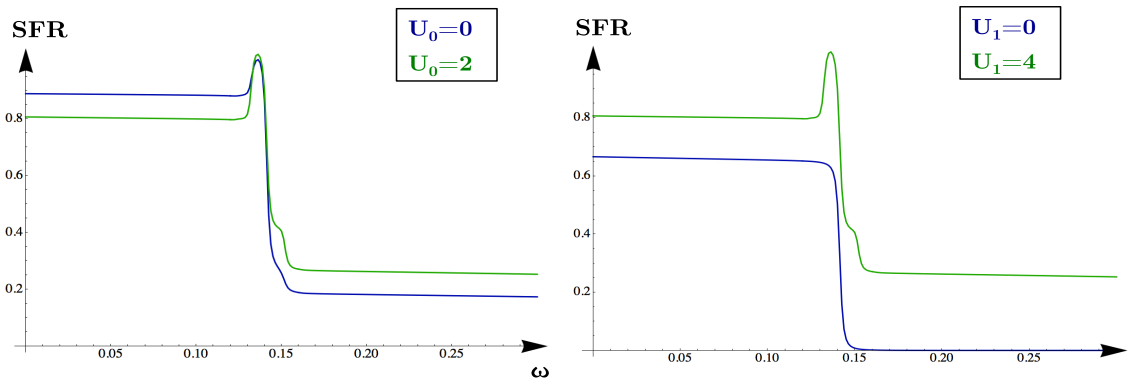

Figure 17: *Left-hand side:* The plot shows the spin-flip-rate (SFR) as a function of the frequency ω with which the underlying magnetic field varies in time for a static potential with zero (blue) and non-zero amplitude (green). The level of the plateaus shifts, but the width of the box is not affected. We set $U_1 = 4$. *Right-hand side:* The spin-flip-rate (SFR) is displayed as a function of the ω for a magnetic impurity with zero (blue) and non-zero amplitude (green). Again, the level of the plateaus shifts, but the width of the box is not affected. We observe that the peak at the end of the box seems to stem from effects caused by the magnetic impurity. For a frequency ω larger than a critical value and for $U_1 = 0$, spin flips no longer occur, the non-magnetic impurity no longer contributes to the spin-flipping processes. We set $U_1 = 2$. For both plots, we set $\mu_B B_0 = 0.001,\ \phi_0 = 0,\ \theta = \pi/2,\ R = 0$.

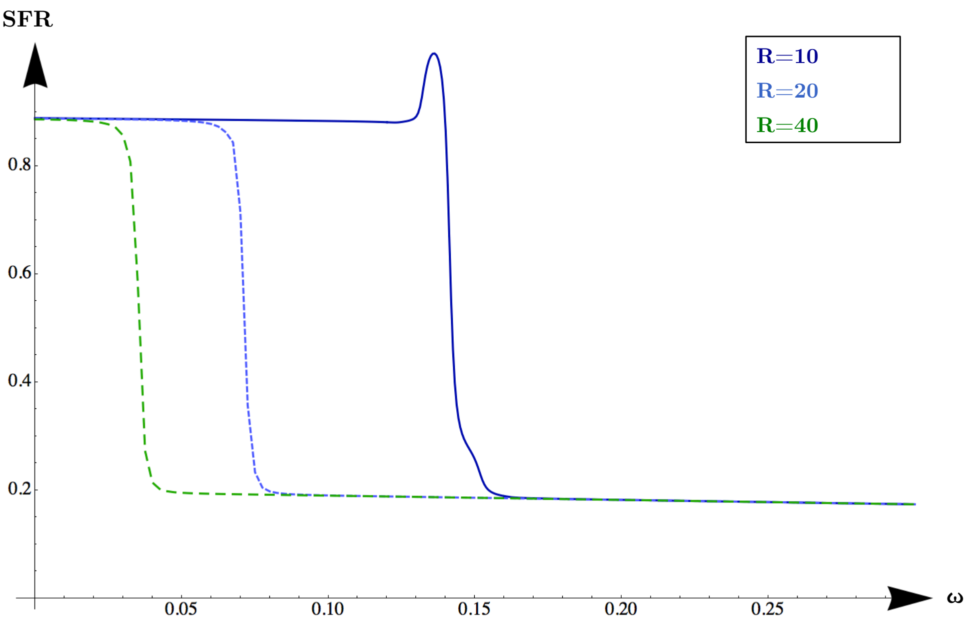

Figure 18: The plot shows the spin-flip-rate (SFR) as a function of the frequency ω with which the underlying magnetic field varies in time for different values of the radius R. For increasing R the width of the box decreases. We set $\mu_B B_0 = 0.001,\ \phi_0 = 0,\ \theta = \pi/2,\ U_1 = 4,\ R = 0,\ U_0 = 0$.

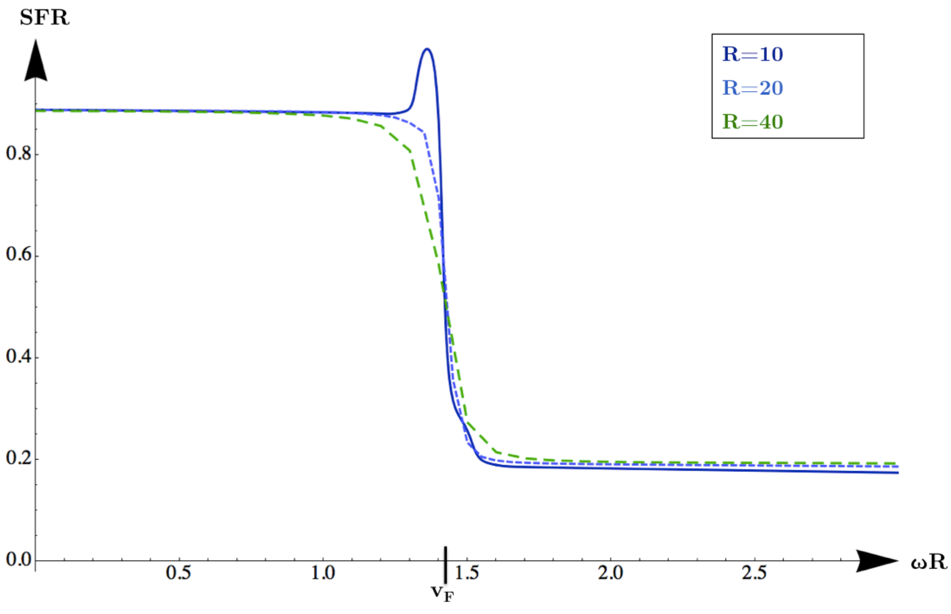

Figure 19: The plot shows the spin-flip-rate (SFR) as a function of the product of the frequency ω with which the underlying magnetic field varies in time and the radius R for different fixed values of R. The width of the box w in plot 18 decreases linear with R, i.e. for a value of R which is twice as high, the box is half as wide, $w \sim R^{-1}$. The edge of the box in this plot is marked by the fermi velocity v_F. We set $\mu_B B_0 = 0.001,\ \phi_0 = 0,\ \theta = \pi/2,\ U_1 = 4,\ U_0 = 0$, so that $v_F = \sqrt{2}$.

6.5 The Rate of Energy Transitions

In this section, we will consider the dependence of the rate of energy transitions on various parameters. We define the rate of energy transitions as the current induced by wave-functions with an energy $\epsilon_n = \epsilon_0 + n\omega$ different from the incoming energy (i.e. $n \neq 0$) divided by the current induced by the incoming wave function, which has the energy ϵ_0.

We define the energy transition rate (ETR) as

$$ETR \equiv \frac{\sum\limits_{n\neq 0} j_n}{j_{in}} \tag{107}$$

where

$$\sum_{n\neq 0} j_n = \sum_{n\neq 0} \left\{ -\left(|r^n_{+l}| \left[\frac{\partial E}{\partial K}\right]^n_{+l} + |r^n_{-l}| \left[\frac{\partial E}{\partial K}\right]^n_{-l} \right) + \left(|t^n_{+r}| \left[\frac{\partial E}{\partial K}\right]^n_{+r} + |t^n_{-r}| \left[\frac{\partial E}{\partial K}\right]^n_{-r} \right) \right\}$$

Firstly, we are again interested in how the energy-transition-rate changes as a function of the radius R. We observe that with increasing radius R, the energy-flip-rate decreases, which is perfectly consistent with our expectations of a system approaching ferromagnetic order. We also observe that for decreasing $|\omega|$ the rate of energy transitions is generally higher. This is consistent with the observations we made in the previous chapter, namely that for small ω the spin-flip-rate increases remarkably. In the case of energy transitions, however, the quantitative significance of these differences is only marginal.

Next, we consider the energy-transition-rate for different choices of the amplitudes of the impurities. For a purely static potential scatterer, no energy transitions occur. For magnetic impurities we observe a high peak in the energy-transition-rate for one particular amplitude of order $5\epsilon_F$, see figure 21. For a magnetic potential barrier which is about as high as the non-magnetic potential, spins are most likely to transition into other energy states. For potentials higher than the fermi energy, the energy-transition-rate decreases dramatically and above a value of approximately $20[\epsilon_F]$, it stays nearly constant, as we have observed before for the spin-flip-rate.

The dependence of the energy transition rate (ETR) on the frequency ω bears some resemblance to the representation of the spin-flip-rate as a function of ω. For large magnetic energies, the energy transition rate is nearly constant, whereas for magnetic energies much smaller than the fermi energy, the energy transition rate has a maximum for small absolute values of ω. What strikes us is the high peak of the ETR for small magnetic fields, which is reminiscent of a resonance peak. Unlike the maximum of the spin-flip-rate however, the maximum peak (and the corresponding 'resonance' frequency) is shifted to the right with respect to the origin. It corresponds to the frequency where before we observed peaks at the margins of the boxes in the STR-plot, see figure 16. In addition, one observes that for large absolute values of the frequency, the energy-transition-rate is once again almost oblivious to possible changes inflicted by higher or lower frequencies.

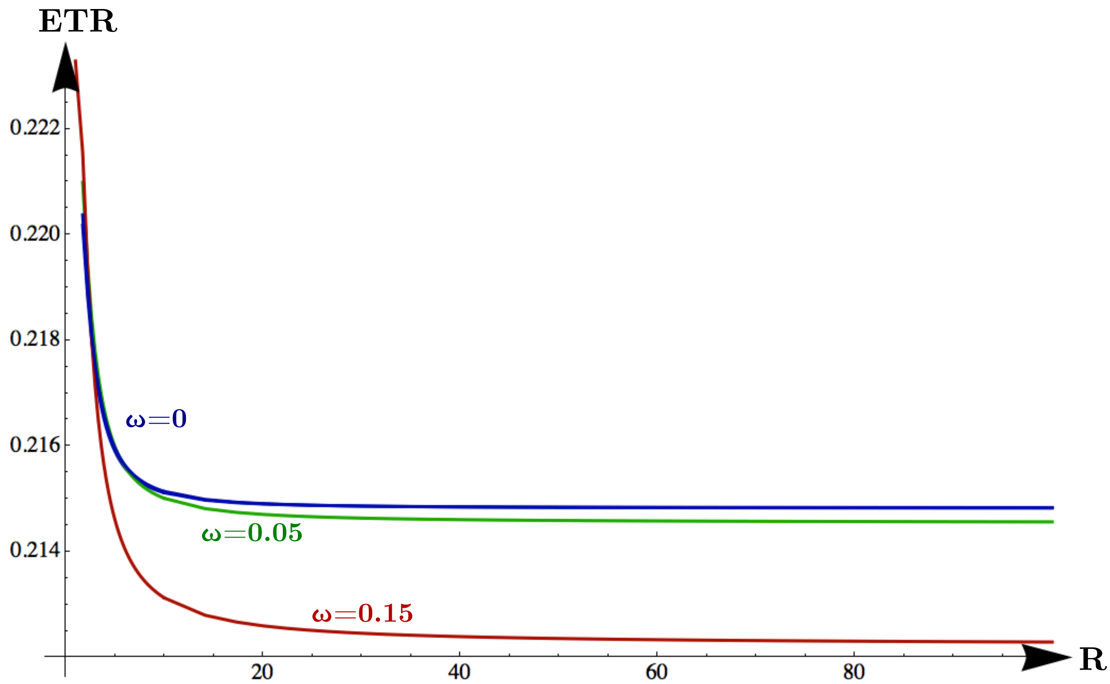

Figure 20: The plot shows the energy-transition-rate (ETR) as a function of the radius of the ring, R, for frequencies $\omega \to 0$ (blue curve) and $\omega = 0.05$ (green curve) and $\omega = 0.15$ (red curve). Surprisingly, the energy transition rate is generally higher for $\omega \to 0$. We also observe the expected tendency of a sinking energy transition rate for a system approaching ferromagnetic order. We chose $\mu_B B_0 = 0.5,\ \phi_0 = 0,\ \theta = \pi/2,\ U_0 = 2,\ U_1 = 4$.

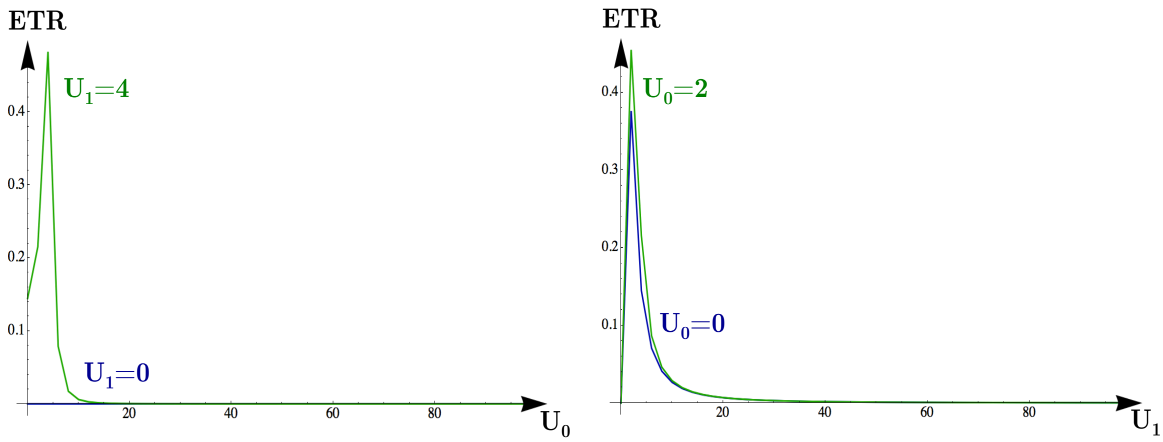

Figure 21: The plot shows the energy-transition-rate (ETR) as a function of the amplitudes of the static and magnetic impurities U_0, U_1. The green curves represent systems where both static and magnetic impurities are present with given non-zero amplitudes, whereas the blue curves show the spin-flip-rate for purely static and magnetic impurities, respectively. We chose $\omega = 0.05,\ \mu_B B_0 = 0.5,\ \phi_0 = 0,\ x = R^2 = 100,\ \theta = \pi/2$.

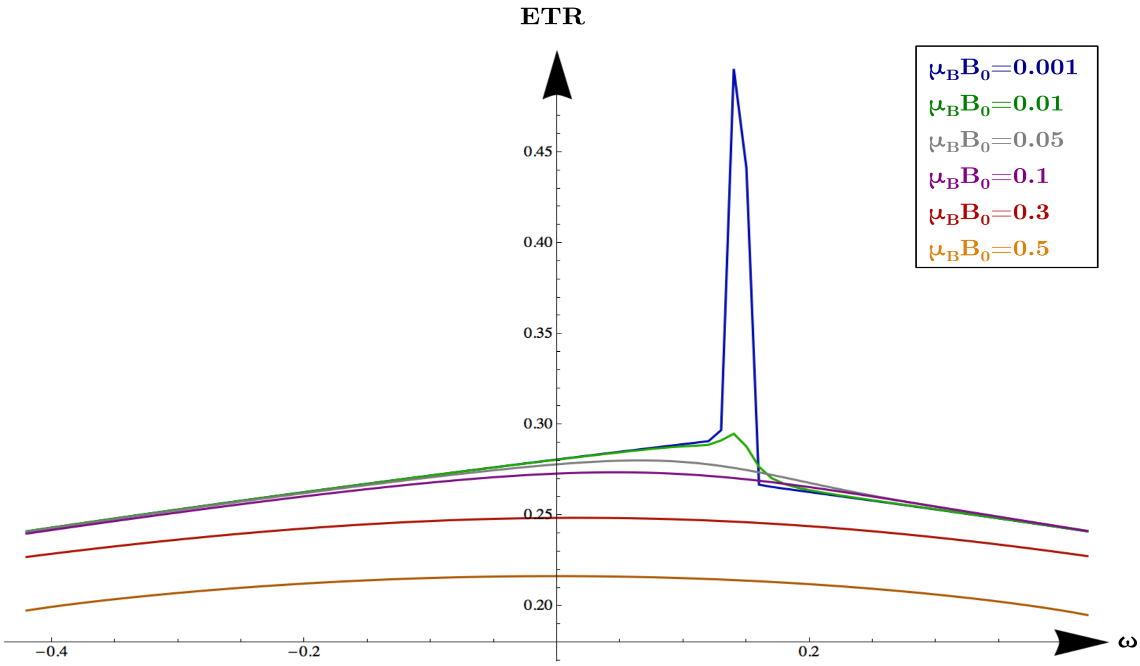

Figure 22: The plot shows the energy-transition-rate (ETR) as a function of the frequency ω with which the underlying magnetic field varies in time. For very small magnetic fields, the energy transition rate is largest. One observes a maximum ETR for a frequency of about 0.15. We chose $\mu_B B_0$ as given in the figure and also set $\phi_0 = 0$, $x = R^2 = 100$, $\theta = \pi/2$, $U_0 = 2$, $U_1 = 4$.

The Average Energy Distance

The average distance in energy covered by a transition into another band can be received by a simple ansatz. The energy difference of a transition from a state with an energy ϵ_0 into a band with energy E^n equals $n \cdot \hbar\omega$. From this we may conclude that the average energy is nothing less than the sum over all n of $n \cdot \hbar\omega$ weighted with the probability of an energy transition into a respective band $\epsilon_0 + n \cdot \hbar\omega$, which corresponds to the sum of all reflection and transmission coefficients with index n. The expectation value of the energy is then given by

$$\langle \Delta \rangle_n = \sum_n \left(\sum_{\sigma=+,-} \sum_{\delta=l,r} (n \cdot \hbar\omega)(|t^n_{\sigma\delta}|^2 + |r^n_{\sigma\delta}|^2) \right) \tag{108}$$

where the index n indicates an averaging over all n. We find that for increasing ω, the average energy distance covered by a transition increases. For the chosen parameters, the curve finds its maximum for $\omega \approx 0.07$. It seems surprising that the average energy does not show symmetry with respect to ω, but steadily decreases for decreasing values of the frequency. However, as we have mentioned before, the system is generally not symmetric, as we chose an incoming wave with a specific direction of propagation and a specific spin state.

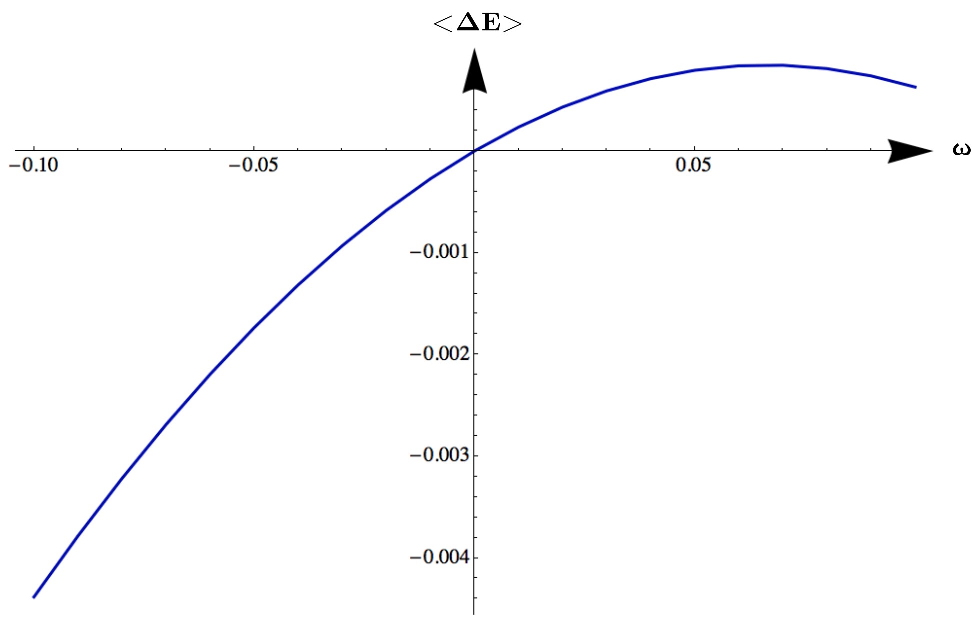

Figure 23: Plot of the average energy distance covered by a transition into another band. The average energy covered has a maximum value for $\omega \approx 0.07$. We chose $\mu_B B_0 = 0.5$, $\phi_0 = 0$, $x = R^2 = 100$, $\theta = \pi/2$, $U_0 = 2$, $U_1 = 4$.

6.6 Transitioning of the Time-Dependent Problem into the Static Problem

Since we considered a time-dependent magnetic order as a variation of a static problem, it goes without saying that we are interested in the way the solutions of both systems blend into one another for $\omega \to 0$.

Both problems produce equal results for a non-magnetic impurity, $U_1 = 0$, and when setting $\omega \to 0$. For a magnetic impurity, which produces energy transitions, the case is not as simple. We have shown that in both cases, we can find the solutions $r^n_{+,l}, r^n_{-,l}, t^n_{+,r}, t^n_{-,r}$ through solving a Matrix equation (compare equation (95)) $\mathbf{Ma} = \mathbf{b}$, where $\mathbf{M}$ is a sum of a diagonal matrix $\mathbf{M}_0$ and a matrix $\tilde{\mathbf{M}}$ representing the terms linear in U_1, which is off-diagonal (diagonal) in the dynamic (static) case.

For small disturbances U_1, we may then write

$$\begin{aligned}\mathbf{a} =&(\mathbf{M}_0 + U_1\tilde{\mathbf{M}})^{-1}\mathbf{b} = (\mathbf{M}_0(1 + U_1\mathbf{M}_0^{-1}\tilde{\mathbf{M}}))^{-1}\mathbf{b}\\ =&(1 + U_1\mathbf{M}_0^{-1}\tilde{\mathbf{M}})^{-1}\mathbf{M}_0^{-1}\mathbf{b} = (\mathbf{M}_0^{-1} - U_1\mathbf{M}_0^{-1}\tilde{\mathbf{M}}\mathbf{M}_0^{-1})\mathbf{b}\end{aligned}$$

where we have used that $(1+x)^{-1} \approx 1-x$ for small x. The term responsible for producing different results for the static and the dynamic problem, even when letting $\omega \to 0$, is the second part of the inversed matrix, $\mathbf{U}_1\mathbf{M}_0^{-1}\tilde{\mathbf{M}}\mathbf{M}_0^{-1}$. The off-diagonal structure of $\tilde{\mathbf{M}}_{dyn}, \tilde{\mathbf{M}}_{stat}$ result in distinct matrix products.

However, one may achieve comparable results when averaging the static results over an angle Ω which has the property that it relates the magnetic impurity to the underlying local magnetic field. The latter should be maximal when perpendicular and minimal when parallel to the direction of magnetization, respectively. From a physical point of view, this corresponds to a rotation of the overall magnetic structure by various angles with respect to the delta potential. We may thus ensure that the direction of the magnetic impurity in relation to the static magnetic order does not have any unintended influence on the result.

Consider a magnetic field $\mathbf{B}_\Omega$ and a general magnetic impurity proportional to $(\mathbf{S}_x, \mathbf{S}_y)^T$ which enclose an angle Ω and let $\omega \ll v_F/R$. The magnetic field is then proportional to

$$\begin{aligned}\mathbf{B}_\Omega =& \begin{pmatrix} \cos\Omega & -\sin\Omega \\ \sin\Omega & \cos\Omega \end{pmatrix} \begin{pmatrix} \mathbf{S}_x \\ \mathbf{S}_y \end{pmatrix} = \begin{pmatrix} \cos\Omega\mathbf{S}_x - \sin\Omega\mathbf{S}_y \\ \sin\Omega\mathbf{S}_x + \cos\Omega\mathbf{S}_y \end{pmatrix}\\ =& \begin{pmatrix} \cos\Omega\left(\frac{\mathbf{S}^+ + \mathbf{S}^-}{2}\right) + i\sin\Omega\left(\frac{\mathbf{S}^+ - \mathbf{S}^-}{2}\right) \\ \sin\Omega\left(\frac{\mathbf{S}^+ + \mathbf{S}^-}{2}\right) - i\cos\Omega\left(\frac{\mathbf{S}^+ - \mathbf{S}^-}{2}\right) \end{pmatrix} = \frac{1}{2}\begin{pmatrix} \mathbf{S}^+e^{i\Omega} + \mathbf{S}^-e^{-i\Omega} \\ -i(\mathbf{S}^+e^{i\Omega} + \mathbf{S}^-e^{-i\Omega}) \end{pmatrix}\end{aligned}$$

Since we observe the same proportionality $\mathbf{S}^+e^{i\Omega} + \mathbf{S}^-e^{-i\Omega}$ for the offdiagonal matrix elements, it becomes clear that the angle Ω is in fact the location of the delta potential, ϕ_0.

Figure 24: The plot shows the spin-flip-rate (SFR) as a function of the angle ϕ_0 for the static problem, which determines the location of the impurity, but also indicates the angle enclosed by the local magnetic field and the field induced by the magnetic impurity. For an angle $\phi_0 = \pi/2$, the spin-flip-rate is maximal, as the magnetic impurity is perpendicular to the local magnetization. By the same logic, we have minima of the spin-flip-rate for integral multiples of π. We also chose $\mu_B B_0 = 0.5$, $\theta = \pi/2$, $x = R^2 = 100$, $U_0 = 2$, $U_1 = 4$.

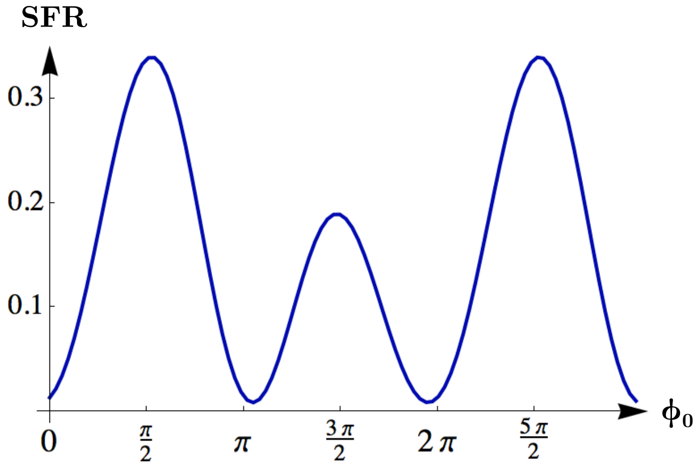

As a result, by varying ϕ_0, we expect to see minima of the spin-flip-rate for $\phi_0 = n\pi$, $n \in \mathbb{Z}$, and maxima for multiples of $\pi/2$, as can be observed in figure 24. We numerically confirmed that the transition of the static problem into the dynamic problem for $\omega \to 0$ holds true for averaging the results received from the dynamic matrix equation over ϕ_0. As an example, the spin-flip-rate as a function of U_0 is given for both matrix equations in figure 25. Note that both curves are in accordance with each other, i.e. averaging over all angles ϕ_0 of the static problem produces the same results as the dynamic problem for $\omega \to 0$.

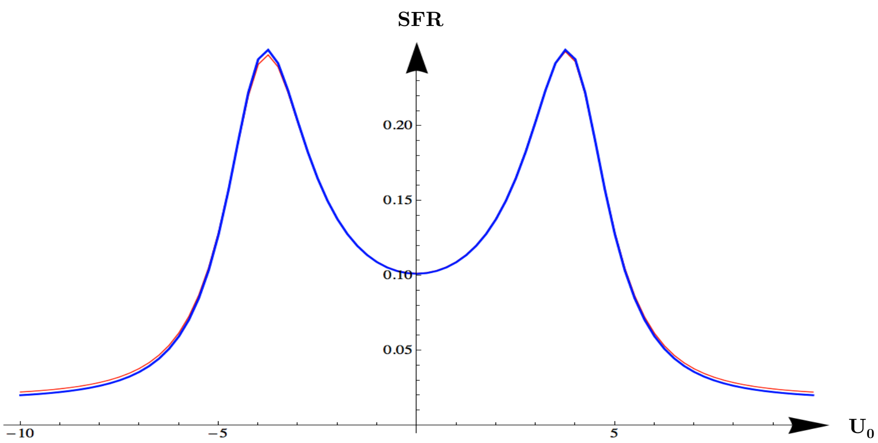

Figure 25: Spin-flip-rate (SFR) as a function of the amplitude of the static impurity U_0 for $U_1 \neq 0$. The red curve corresponds to the data generated by the static matrix equation averaged over all ϕ_0, whereas the blue curve shows the results for a matrix equation including off-diagonal terms, where $\omega \to 0$. Both curves are, neglecting numerical inaccuracies, in perfect accordance with each other. We chose $\mu_B B_0 = 0.5$, $\phi_0 = 0$, $x = R^2 = 100$, $\theta = \pi/2$, $U_1 = 4$.

7 Conclusion and Outlook

In this Bachelor Thesis, we have studied the interplay of magnetism and electric current by considering the effects of a one-dimensional, non-collinear magnetic structure with a time-dependence on a passing electron moving on a ring.

We analytically determined the exact wave function of a particle moving through a non-collinear time-dependent magnetic field, which is the product of a time-dependent and an angle-dependent function and we computed the eigenvalues of a transformed Hamiltonian, which may be interpreted as eigenenergies.

We also confirmed that the motion of a spin-$\frac{1}{2}$-electron through the chosen magnetic field is an adiabatic problem by showing that the exact eigenenergies in the limit of an infinite radius of the ring are in accordance with the eigenenergies emerging from an adiabatic ansatz. We found that for a time-dependence of the position of the electron, there are no emergent electric fields since the undisturbed Hamiltonian can be mapped onto a time-independent one by unitary transformations.

Finally, we investigated the effects of a defect in our set-up by introducing a magnetic impurity into the system, which breaks Galilei invariance and energy conservation. We saw that the spin-flip-rate and the rate of energy transitions of an incoming particle wave resulting from the scattering by the potential decrease for increasing adiabaticity of the problem. We also found that the magnetic impurity is responsible for most spin-flipping processes. For small absolute values of ω, both the energy transition rate and the spin-flip-rate have a maximum and both are relatively indifferent to change of ω outside of that area of frequencies. We numerically confirmed that the dynamic problem can be mapped onto the static problem, but only if one averages the static results over all possible angles ϕ_0 enclosed by the direction of magnetization and the magnetic impurity and considering the limit of $\omega \to 0$.

With a view to future projects, it will be interesting to consider a similar problem where the parameter determining the direction of magnetization is time-dependent, $\tilde{\theta} = \theta - \omega t$. In this case, Galilei transformations of the undisturbed Schroedinger equation will presumably no longer leave the problem invariant, and electric fields will emerge.

List of Figures

References

[1] S. Mühlbauer, *et al.* “Skyrmion Lattice in a Chiral Magnet.” Science **323** (2009).

[2] C. Pfleiderer, *et al.* “Quantum order in the chiral magnet MnSi.” Journal of Physics: Condensed Matter **21**, 164215 (2009).

[3] C. Pfleiderer. “Magnetismus mit Drehsinn.” Physik Journal **9**, 25–30 (2010).

[4] A. Bauer, *et al.* “Quantum phase transitions in single-crystal $Mn_{1-x}Fe_xSi$ and $Mn_{1-x}Co_xSi$: Crystal growth, magnetization, ac susceptibility, and specific heat.” Phys. Rev. B **82**, 064404 (2010).

[5] S. Seki, X. Z. Yu, S. Ishiwata, and Y. Tokura. “Observation of Skyrmions in a Multiferroic Material.” Science **336**, 198 (2012).

[6] T. Adams, *et al.* “Long wavelength helimagnetic order and skyrmion lattice phase in Cu_2OSeO_3.” arXiv:1204.3597v1 (2012).

[7] X. Z. Yu, *et al.* “Real-Space Observation of a Two-Dimensional Skyrmion Crystal.” Nature **465**, 901 (2010).

[8] X. Z. Yu, *et al.* “Near room-temperature formation of a skyrmion crystal in thin-films of the helimagnet FeGe.” Nat. Mat. **10**, 106 (2011).

[9] J. Zang, M. Mostovoy, J. H. Han, and N. Nagaosa. “Dynamics of Skyrmion Crystals in Metallic Thin Films.” Phys. Rev. Lett. **107**, 136804 (2011).

[10] G. Tatara, *et al.* “Spin torque and force due to current for general spin textures.” J. Phys. Soc. Jpn. **76**, 054707 (2007).

[11] P. Bruno, V. K. Dugaev, and M. Taillefumier. “Topological Hall Effect and Berry Phase in Magnetic Nanostructures.” Phys. Rev. Lett. **93**, 096806 (2004).

[12] S. A. Yang, *et al.* “Universal Electromotive Force Induced by Domain Wall Motion.” Phys. Rev. Lett. **102**, 067201 (2009).

[13] C. Pfleiderer and A. Rosch. “Condensed-matter physics: Single skyrmions spotted.” Nature (2010).

[14] A. Neubauer, *et al.* “Topological Hall Effect in the *A* Phase of MnSi.” Phys. Rev. Lett. **102**, 186602 (2009).

[15] K. Everschor. *Current-Induced Dynamics of Chiral Magnetic Structures*. Ph.D. thesis, University of Cologne (2012).

[16] F. Jonietz, *et al.* “Spin Transfer Torques in MnSi at Ultra-low Current Densities.” Science **330**, 1648 (2010).

[17] T. Schulz, *et al.* "Emergent electrodynamics of skyrmions in a chiral magnet." Nat. Phys. **8**, 301 (2012).

[18] M. Baedorf. *Berry-Phase und Spinstreuung.* Bachelor's thesis, University of Cologne (2011).

[19] M. Berry. "Quantal phase factors accompanying adiabatic changes." Proceedings of the Royal Society A 392, 45-57 (1984).

[20] M. S. Sarandy, L.-A. Wu, and D. A. Lidar. "Consistency of the Adiabatic Theorem." Quantum Information Processing **3**, 333 (2004). ISSN 1570-0755.

[21] D. Xiao, M.-C. Chang, and Q. Niu. "Berry phase effects on electronic properties." Rev. Mod. Phys. **82**, 1959–2007 (2010).

[22] A. Rosch and A. Weinkauf. "Quantenphysik." (2008). Lecture notes.

[23] M. Moskalets and M. Büttiker. "Floquet scattering theory of quantum pumps." Phys. Rev. B **66**, 205320 (2002).

[24] J. H. Shirley. "Solution of the Schrödinger Equation with a Hamiltonian Periodic in Time." Phys. Rev. **138**, B979–B987 (1965).

Thanks and Acknowledgements

First of all, I would like to thank Prof. Dr. Achim Rosch for his excellent supervision of my Bachelor Thesis and for always taking time to answer my questions. I appreciate immensely the insight he offered me into up-to-date topics of physical research and I would like to thank him for the enthusiasm he shows when tackling problems, which I found infectious.

Special thanks go to Karin Everschor for her most helpful advice and kind guidance as well as her careful proof-reading. I am very grateful for her always making time for my questions. I highly value our fruitful discussions and her helpful suggestions for improvements. I would also like to acknowledge the support from Matthias Sitte, who kindly assisted me with numerical problems.

Finally, I am very grateful to all members of the group for providing a very pleasant and friendly working atmosphere and giving me an insight into their personal areas of research through regular talks, which I found most inspiring to listen to.

I further wish to express my thanks to the 'Studienstiftung des deutschen Volkes', Prof. Dr. Thomas Szyperski (Department of Chemistry, University at Buffalo, The State University of New York) and the Department for Innovation, Science and Research of the State NRW for financially supporting my Bachelor studies.

Declaration

I hereby declare that this thesis is my own work and effort. I further declare that to the best of my knowledge and belief all external authorships have been marked as such and all other sources of information have been acknowledged.

Sarah Maria Schroeter

Cologne, July 6th 2012